Sequential Dehydrogenative Borylation/Hydrogenation Route to Polyethyl-Substituted, Weakly Coordinating Carborane Anions

Eduardo Molinos, Simon K. Brayshaw, Gabriele Kociok-Köhn, and Andrew S. Weller*

Department of Chemistry, University of Bath, Bath BA2 7AY, U.K.

Received January 16, 2007

Treatment of $Rh(PPh_3)_2$(1-H-*closo*-$CB_{11}H_{11}$) with ethene results in dehydrogenative borylation to form the vinyl−borate complex $Rh(PPh_3)_2$(1-H-7/12-(H_2C═CH)-*closo*-$CB_{11}H_{10}$) as a mixture of 7- and 12-isomers. Further dehydrogenative borylation does not occur; this is accounted for by the strong binding of the vinylcarborane to the $\{Rh(PPh_3)_2\}^+$ fragment through C═C and B−H interactions. Addition of H_2 results in hydrogenation of the vinyl group and the quantitative formation of the *B*-ethylcarborane complex $Rh(PPh_3)_2$(1-H-7/12-(Et)-*closo*-$CB_{11}H_{10}$). The crystal structure of the norbornadiene adduct of one the isomers, $[Rh(PPh_3)_2(nbd)]$[1-H-12-(H_2C═CH)-*closo*-$CB_{11}H_{10}$], has been determined. Addition of ethene to the complex $Rh(PPh_3)_2$(1-H-12-Br-*closo*-$CB_{11}H_{10}$), in which the 12-position on the cage is blocked, results in only one isomer: $Rh(PPh_3)_2$(1-H-7-(CH_2═CH)-12-Br-*closo*-$CB_{11}H_9$). Sequential addition of ethene/H_2 to $Rh(PPh_3)_2$(1-H-7/12-(Et)-*closo*-$CB_{11}H_{10}$) results, after six cycles, in the pentaethyl-substituted complex (characterized as the nbd salt) $[Rh(PPh_3)_2(nbd)]$[1-H-2,4,8,10,12-$(Et)_5$-*closo*-$CB_{11}H_6$]. The solid-state structure shows that the antipodal boron vertex, two lower pentagonal belt vertices, and two upper-belt vertices have been functionalized, with no two adjacent vertices on the same pentagonal belt substituted. The degree of ethylation can be controlled. Replacing the hydrogen on the cage carbon with a bulkier substituent (methyl or Si^iPr_3) affords products in which only three B−H vertices have been substituted, and the solid-state structure of $Rh(PPh_3)_2$(1-Me-7,11,12-$(Et)_3$-*closo*-$CB_{11}H_8$) shows that the antipodal boron vertex and two lower pentagonal belt vertices have undergone dehydrogenative borylation. Mechanistic insight into the dehydrogenative borylation comes from addition of D_2 to a CH_2Cl_2 solution of $Rh(PPh_3)_2$(*closo*-$CB_{11}H_{12}$), which results in H/D exchange of the B−H vertices, suggesting that the metal fragment reversibly inserts into a B−H bond of the cage anion to form a boryl species. Attempts to observe intermediates in the actual hydroboration process by addition of ethene to $Rh(PPh_3)_2$(1-H-*closo*-$CB_{11}H_{11}$) resulted in the observation of the tris(ethene) complex $[Rh(PPh_3)_2(\eta^2\text{-}C_2H_4)_3]$[1-H-*closo*-$CB_{11}H_{11}$], which has been characterized crystallographically as the [*closo*-$CB_{11}H_6Br_6$] salt.

Introduction

Within the landscape of metal catalysis, transformations mediated by cationic transition-metal centers occupy an important position. Such metal centers need to be partnered with anions, and the role of the anion in influencing the rate of the reaction, the stability of the catalyst, and even product distributions is now widely recognized, especially the influence that the so-called weakly coordinating anions have on catalytic systems.[1−4] Central to the development of weakly coordinating anions have been the carborane anions based upon [1-*closo*-$CB_{11}H_{11}]^-$ (Chart 1).[5,6] When surrounded by halogens, e.g., [1-H-*closo*-$CB_{11}Cl_{11}]^-$, these anions complement other weakly coordinating or noncoordinating anions such as $[BAr^F{}_4]^-$ ($BAr^F{}_4$ = $B\{C_6H_3(CF_3)_2\}_4$) and $[Al(OC(CF_3)_3)_4]^-$ [7] and in particular show impressive chemical resistance to decomposition or oxidation.[6,8] A particularly interesting subset of the carborane monoanions are those surrounded by alkyl groups, such as [*closo*-$CB_{11}Me_{12}]^-$ (Chart 1), accessed by electrophilic substitution of the {BH} vertices in the parent [*closo*-$CB_{11}H_{12}]^-$ anion

Chart 1

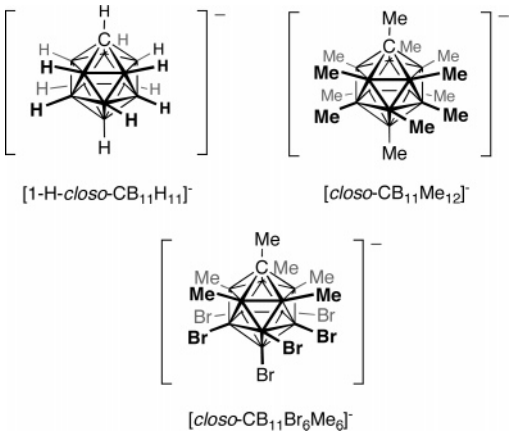

* To whom correspondence should be addressed. E-mail: a.s.weller@bath.ac.uk.

(1) Macchioni, A. *Chem. Rev.* **2005**, *105*, 2039−2073.
(2) Chen, E. Y. X.; Marks, T. J. *Chem. Rev.* **2000**, *100*, 1391−1434.
(3) Pregosin, P. S.; Kumar, P. G. A.; Fernández, I. *Chem. Rev.* **2005**, *105*, 2977−2998.
(4) Krossing, I.; Raabe, I. *Angew. Chem., Int. Ed.* **2004**, *43*, 2066.
(5) Reed, C. A. *Acc. Chem. Res.* **1998**, *31*, 133−139.
(6) Reed, C. A. *Chem. Commun.* **2005**, 1669−1677.
(7) Krossing, I.; Raabe, I. *Angew. Chem., Int. Ed.* **2004**, *43*, 2066−2090.
(8) Kato, T.; Stoyanov, E.; Geier, J.; Grutzmacher, H.; Reed, C. A. *J. Am. Chem. Soc.* **2004**, *126*, 12451−12457.

10.1021/om070043p CCC: $37.00 © 2007 American Chemical Society
Publication on Web 03/28/2007

Scheme 1

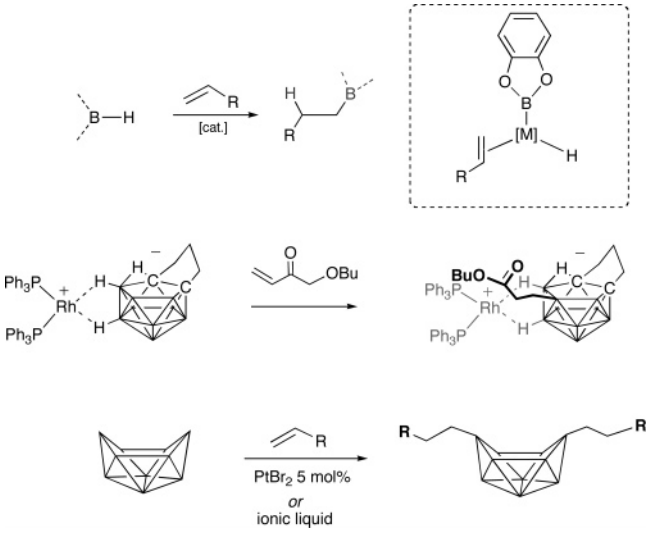

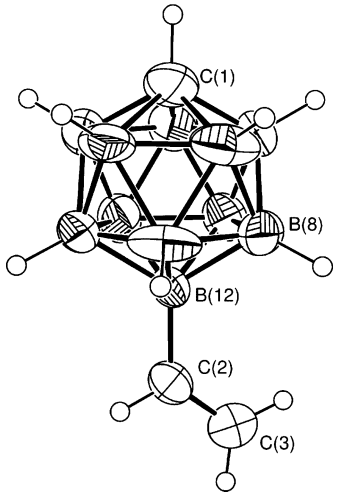

Figure 1. Solid-state structure of the anionic portion of **2a**. The $[Rh(PPh_3)_2(nbd)]^+$ cation is not shown. Thermal ellipsoids are shown at the 50% probability level.

using methyl triflate.[9−11] Although these monoanions are less stable than their halogenated counterparts with respect to B−Me cleavage by strong acids or electrophiles,[12−14] they can possess the very attractive properties of showing appreciable solubility as their lithium salts in low-dielectric solvents such as hexane. When partnered with main-group or d-block metal cations, they can also show intermolecular M···H_3C interactions which have relevance to C−H activation processes and metal alkane complexes.[15,16] Extending the range of alkyl-substituted carborane monoanions by functionalization of the B−H vertices in [*closo*-$CB_{11}H_{12}]^-$ with alkyl groups other than methyl has proved to be problematic. There is a single report of perethylation using EtBr, but this uses conditions that are not necessarily suitable for large-scale synthesis (sealed tube, 220 °C).[17] Arylation of iodo-substituted monocarboranes using palladium cross-coupling with aryl Grignards has been reported,[11,18,19] but this leads to functionalized carboranes that are not ideally set up for use as weakly coordinating anions, due to the arene groups that are well-established to coordinate to metal centers. Cage-carbon functionalization is easier, given the ease of deprotonation of the C−H group and subsequent nucleophilic substitution strategies.[11,20] Although per-{BH} substitution is not well established outside methylation, peralkylation of [*closo*-$B_{12}(OH)_{12}]^{2-}$ with R−X at elevated temperatures leads to a variety of ether-linked closomers in good yield.[21]

Transition-metal-mediated catalytic borylation of alkenes using simple boron sources (e.g., $HB(OR)_2$) is well-known (Scheme 1, top).[22−24] With polyboranes, Sneddon[25−31] and Hawthorne[32] have shown that one or two {BH} vertices on, for example, *arachno*-$B_{10}H_{14}$, [*nido*-7,8-$C_2B_9H_{12}]^-$, or borazines can be alkylated using transition-metal catalysts such as the $\{Rh(PPh_3)_2\}^+$ fragment, $Cp_2Ti(CO)_2$, and $PtBr_2$ (Scheme 1, bottom), although recent work has shown that the use of ionic liquids removes the necessity of the metal catalyst in some systems.[33] Given this precedent, we speculated whether such routes could be extended to [1-H-*closo*-$CB_{11}H_{11}]^-$ to effect multiple substitutions of the anion with alkenes, thus leading to polyalkyl-substituted carborane monoanions with potentially interesting properties as weakly coordinating anions. We report here that the sequential, and regioselective, functionalization of [1-H-*closo*-$CB_{11}H_{11}]^-$ with up to five ethyl groups under mild conditions can be achieved using $\{Rh(PPh_3)_2\}^+$ fragments as catalysts but further substitution is disfavored by increasing steric hindrance. We also comment on the mechanistic aspects of this process and describe an unstable intermediate ethene complex

(9) King, B. T.; Janousek, Z.; Gruner, B.; Trammell, M.; Noll, B. C.; Michl, J. *J. Am. Chem. Soc.* **1996**, *118*, 3313−3314.
(10) Vyakaranam, K.; Janousek, Z.; Eriksson, L.; Michl, J. *Heteroat. Chem.* **2006**, *17*, 217−223.
(11) Korbe, S.; Schreiber, P. J.; Michl, J. *Chem. Rev.* **2006**, *106*, 5208−5249.
(12) King, B. T.; Zharov, I.; Michl, J. *Chem. Innovation* **2001**, 23−31.
(13) Zharov, I.; Havlas, Z.; Orendt, A. M.; Barich, D. H.; Grant, D. M.; Fete, M. G.; Michl, J. *J. Am. Chem. Soc.* **2006**, *128*, 6089−6100.
(14) Ingleson, M. J.; Kociok-Kohn, G.; Weller, A. S. *Inorg. Chim. Acta* **2005**, *358*, 1571−1580.
(15) Zharov, l.; Weng, T.-C.; Orendt, A. M.; Barich, D. H.; Penner-Hahn, J.; Grant, D. M.; Havlas, Z.; Michl, J. *J. Am. Chem. Soc.* **2004**, *126*, 12033−12046.
(16) Ingleson, M. J.; Patmore, N. J.; Kociok-Köhn, G.; Mahon, M. F.; Ruggiero, G. D.; Weller, A. S.; Clarke, A. J.; Rourke, J. P. *J. Am. Chem. Soc.* **2004**, *126*, 1503−1517.
(17) Tsang, C. W.; Xie, Z. W. *Chem. Commun.* **2000**, 1839−1840.
(18) Franken, A.; Kilner, C. A.; Thornton-Pett, M.; Kennedy, J. D. *Chem. Commun.* **2002**, 2048−2049.
(19) Franken, A.; Kilner, C. A.; Thornton-Pett, M.; Kennedy, J. D. *Collect. Czech. Chem. Commun.* **2002**, *67*, 869−912.
(20) Jelinek, T.; Baldwin, P.; Scheidt, W. R.; Reed, C. A. *Inorg. Chem.* **1993**, *32*, 1982−90.
(21) Farha, O. K.; Julius, R. L.; Lee, M. W.; Huertas, R. E.; Knobler, C. B.; Hawthorne, M. F. *J. Am. Chem. Soc.* **2005**, *127*, 18243−18251.
(22) Irvine, G. J.; Lesley, M. J. G.; Marder, T. B.; Norman, N. C.; Rice, C. R.; Robins, E. G.; Roper, W. R.; Whittell, G. R.; Wright, L. J. *Chem. Rev.* **1998**, *98*, 2685−2722.
(23) Burgess, K.; Vanderdonk, W. A.; Westcott, S. A.; Marder, T. B.; Baker, R. T.; Calabrese, J. C. *J. Am. Chem. Soc.* **1992**, *114*, 9350−9359.
(24) Mannig, D.; Noth, H. *Angew. Chem., Int. Ed.* **1985**, *24*, 878−879.
(25) Wilczynski, R.; Sneddon, L. G. *Inorg. Chem.* **1981**, *20*, 3955−3962.
(26) Davan, T.; Corcoran, E. W.; Sneddon, L. J. *Organometallics* **1983**, *2*, 1693−1694.
(27) Lynch, A. T.; Sneddon, L. G. *J. Am. Chem. Soc.* **1989**, *111*, 6201−6209.
(28) Mazighi, K.; Caroll, P. J.; Sneddon, L. G. *Inorg. Chem.* **1993**, *32*, 1963−1969.
(29) Kadlecek, D. E.; Carroll, P. J.; Sneddon, L. G. *J. Am. Chem. Soc.* **2000**, *122*, 10868−10877.
(30) Pender, M. J.; Carroll, P. J.; Sneddon, L. G. *J. Am. Chem. Soc.* **2001**, *123*, 12222−12231.
(31) Wei, X. L.; Carroll, P. J.; Sneddon, L. G. *Organometallics* **2004**, *23*, 163−165.
(32) Hewes, J. D.; Kreimendahl, C. W.; Marder, T. B.; Hawthorne, M. F. *J. Am. Chem. Soc.* **1984**, *106*, 5757−5759.
(33) Kusari, U.; Li, Y. Q.; Bradley, M. G.; Sneddon, L. *J. Am. Chem. Soc.* **2004**, *126*, 8662−8663.

Scheme 2 [a]

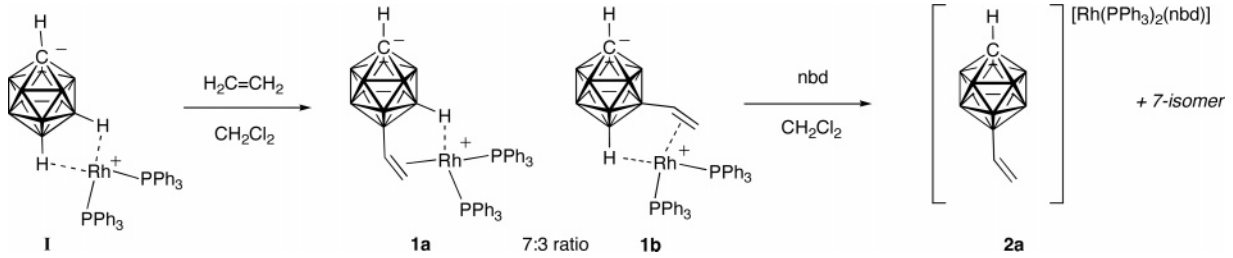

[a] Hydrogen atoms on B−H vertices are only shown when they are coordinated to the metal.

Scheme 3 [a]

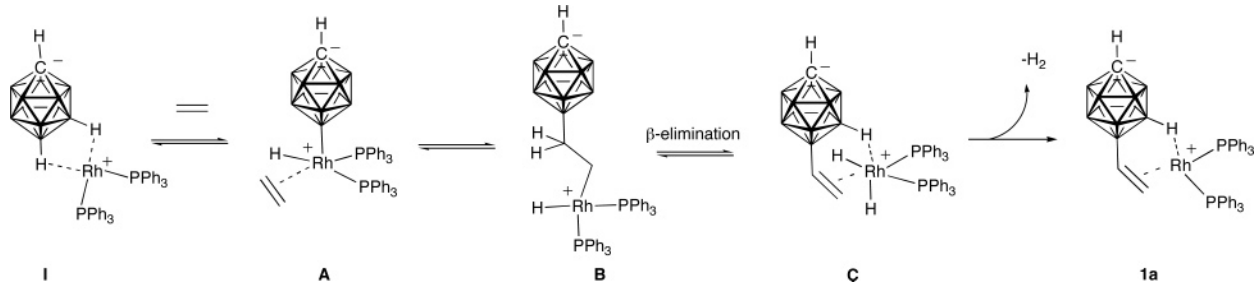

[a] Only the 12-isomer is shown.

Scheme 4 [a]

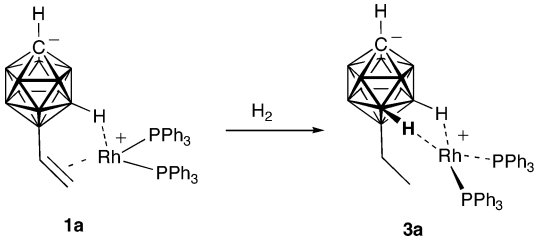

[a] Only the 12-isomer is shown.

characterized by spectroscopic and crystallographic techniques. Aspects of the work have been communicated previously.[34]

Results and Discussion

Sequential Dehydrogenative Borylation Reactions. We have previously reported the complex $Rh(PPh_3)_2$(1-H-*closo*-$CB_{11}H_{11}$) (**I**; Scheme 2), in which the metal fragment interacts with the carborane through two, lower hemisphere {BH} vertices.[35] Addition of D_2 (1 atm) to **I** in CD_2Cl_2 solution in a NMR tube resulted in the gradual (days) H/D exchange at the {BH} vertices, as evidenced by the disappearance of BH signals in the $^1H\{^{11}B\}$ NMR spectrum and the loss of B−H coupling in the ^{11}B NMR spectrum. Speculating that the H/D exchange process most probably occurs via reversible insertion of the metal fragment into a B−H bond of the carborane, leading to a putative hydrido−boryl intermediate (e.g., Scheme 1, top), and that such an intermediate is well set up for hydroboration of an alkene by the cage, we added a range of alkenes to **I**. Although a selection of alkenes (ethene, 1-hexene, *tert*-butylethene, butyl acrylate) did undergo hydroboration to afford the corresponding functionalized borane cages, only ethene resulted in the compositionally purest products. Other olefins gave mixtures of multiply substituted cage anions as determined by ESI-MS and were not studied in detail. Other catalysts that have proved useful in the past led to either a mixture of products ($PtBr_2$ or $PdBr_2$) or no reaction ($Cp_2Ti(CO)_2$).[25−31]

Addition of excess ethene to **I** in CH_2Cl_2 solution at room temperature for 15 h affords the vinyl complex $Rh(PPh_3)_2$(1-H-(H_2C═CH)-*closo*-$CB_{11}H_{10}$) (**1**) in reasonable isolated yield (61%), although as monitored by in situ NMR spectroscopy the conversion is essentially quantitative. Compound **1** arises from dehydrogenative borylation of ethene. No reaction is observed between ethene and [1-H-*closo*-$CB_{11}H_{11}]^-$. NMR spectroscopy shows that this compound is formed as a mixture of two isomers: $Rh(PPh_3)_2$(1-H-12-(H_2C═CH)-*closo*-$CB_{11}H_{10}$) (**1a**) and $Rh(PPh_3)_2$(1-H-7-(H_2C═CH)-*closo*-$CB_{11}H_{10}$) (**1b**). These two compounds are formed in a 7:3 ratio on the basis of relative integrals in the ^1H and ^{11}B NMR spectra. Both isomers show three separate vinylic resonances in the ^1H NMR spectrum, between δ 4.95 and 2.56, which were aided in their identification by $^1H-^1H$ COSY experiments. These vinylic signals are shifted to high field compared to $[Rh(PPh_3)_2(nbd)][1\text{-H-7/12-}(H_2C$═CH)-*closo*-$CB_{11}H_{10}]$ (**2a**,**b**), complexes in which the metal fragment is not associated with the cage anion (vide infra), indicative of coordination of the C═C bond to the metal center in **1a**,**b**.[36,37] The high-field region of the $^1H\{^{11}B\}$ NMR spectrum shows broad peaks characteristic of Rh−*H*−B interactions between δ −0.80 and −2.15,[38] which broaden considerably in the ^1H NMR spectrum due to coupling to quadrupolar boron. Overall, these data suggest a solution structure in which the $\{Rh(PPh_3)_2\}^+$ fragment in each isomer binds to the *B*-vinyl group of the cage and one B−H vertex through a three-center−two-electron interaction.

The presence of a *B*-vinyl group was ultimately confirmed by an X-ray diffraction study of **2a**, $[Rh(PPh_3)_2(nbd)][1\text{-H-12-}(H_2C$═CH)-*closo*-$CB_{11}H_{10}]$, which is formed on addition of norbornadiene (nbd) to a CH_2Cl_2 solution of **1a**,**b** to afford **2a**,**b**, from which crystals of **2a** could be isolated. The ^1H NMR data

(34) Molinos, E.; Kociok-Kohn, G.; Weller, A. S. *Chem. Commun.* **2005**, 3609−3611.

(35) Rifat, A.; Patmore, N. J.; Mahon, M. F.; Weller, A. S. *Organometallics* **2002**, *21*, 2856−2865.

(36) Crabtree, R. H. *The Organometallic Chemistry of the Transition Metals*; Wiley: Hoboken, NJ, 2005.

(37) Du, S.; Ellis, D. D.; Jelliss, P. A.; Kautz, J. A.; Malget, J. M.; Stone, F. G. A. *Organometallics* **2000**, *19*, 1983−1992.

(38) Rifat, A.; Laing, V. E.; Kociok-Kohn, G.; Mahon, M. F.; Ruggiero, G. D.; Weller, A. S. *J. Organomet. Chem.* **2003**, *680*, 127−135.

Scheme 5

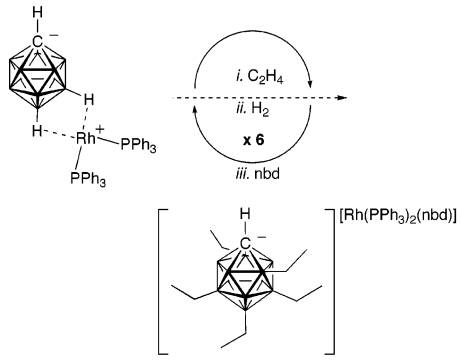

7

of the mixture **2** show the same ratio of vinyl protons, but these are now observed between δ 6.35 and 5.18, while the $^1H\{^{11}B\}$ NMR spectrum no longer shows distinctive Rh−*H*−B resonances at high field—all indicating that the metal fragment is not interacting with the cage anion. In the ^{11}B NMR spectrum, multiple environments are observed, and a $^{11}B-^{11}B$ COSY experiment allowed cage anions with approximate C_{5v} symmetry (**2a**) and C_s symmetry (**2b**) to be identified. The relative ratio of these two species in the ^{11}B NMR spectrum is ∼7:3, which mirrors that found in the ^1H NMR spectrum and allows the vinylic protons to be identified with a particular isomer. The solid-state structure of the anion in **2a** is shown in Figure 1. Although differentiation between cage carbon and boron atoms by X-ray diffraction can be problematic, the B−C distances (1.656(5)−1.719(6) Å) in **2a** all being shorter than the other B−B distances (1.727(5)−1.829(6) Å) in the cage is a good indicator that the cage carbon atom was reliably located and indicates 12-substitution on the cage. However, without a labeled vertex (e.g, C_{cage}−Me) this assignment must be treated with a degree of caution, especially given the existence of both 7- and 12-isomers in solution. A short C(2)−C(3) distance (1.323(4) Å) is consistent with a vinyl group. The associated B(12)−C(2) bond length of 1.583(4) Å is longer than those in the alkenyl-substituted carborane 7-($CH_2(CH_2)_2CH$═CH)-*arachno*-6,8-$C_2B_7H_{12}$ (1.546(2) Å),[29] in which there is suggested to be a π-bonding component to the interaction between the boron and vinyl atoms, reminiscent of conjugated olefins. In the case of **2a** we suggest no such bonding is present, on the basis of the long B−C bond length and the short C(2)−C(3) distance for the vinyl group. Indeed, the B−C distance is similar to that reported for *B*-methyl groups in methylated carborane monoanions[9,16] and those observed in the ethyl-substituted carborane **7** (vide infra).

Compounds **1a**,**b** (and derivatives **2a**,**b**) result from dehydrogenative borylation of ethene by [1-H-*closo*-$CB_{11}H_{11}]^-$ mediated by an exo-coordinated $\{Rh(PPh_3)_2\}^+$ fragment, which occurs by β-elimination from the insertion product of ethene into the Rh−boryl bond (Scheme 3). Transition-metal-mediated catalytic dehydrogenative borylation of alkenes using simple boron sources is well established,[25,39,40] and Sneddon has previously commented on such a process occurring during monofunctionalization of boranes, carboranes, and borazines with 1-alkenes using transition-metal catalysts such as $PdBr_2$ and $PtBr_2$ as the hydroboration mediator.[26,27,29] It has been suggested that dehydrogenative borylation occurs in preference

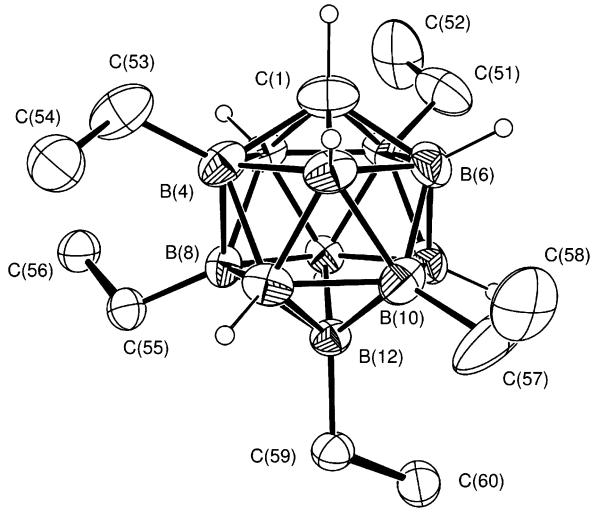

Figure 2. Solid-state structure of the anionic portion of **7**. The $[Rh(PPh_3)_2(nbd)]^+$ cation is not shown. Thermal ellipsoids are shown at the 30% probability level. The minor disordered components of the ethyl groups have been omitted for clarity.

to reductive elimination of alkyl borate (which would result in hydroboration) when steric bulk forces the metal alkyl to adopt a geometry that favors β-elimination. Coordinating solvents, such as acetonitrile, also disfavor reductive elimination and favor β-elimination.[40] The bulky carborane anion in **1** fulfils the first criterion, while the large excess of ethene present might also disfavor reductive elimination by filling a vacant site and also removing the H_2 liberated by β-elimination, by the formation of ethane. The 12-/7-substitution pattern is also consistent with initial insertion of the $\{Rh(PPh_3)_2\}^+$ fragment into the most electron-rich B−H vertices at the bottom of the cage.[15,41] *B*-Vinyl-substituted carboranes have been reported previously as arising from cross-coupling reactions between *B*-halide cages and vinyl Grignards or zinc reagents[42−44] or by metal-mediated B−H insertion of an alkyne into a metallacarborane.[37]

Electrospray ionization mass spectrometry (ESI-MS—see the Supporting Information) also shows that by far the major product is the one that arises from dehydrogenative borylation (*m*/*z* 169.3). However, there is also a small amount of cage anion that has a mass envelope (*m*/*z* 196.2) which indicates a further B−H substitution has occurred to afford the mixed ethylvinylcarborane anion [1-H-(CH_3CH_2)(CH_2═CH)-*closo*-$CB_{11}H_9]^-$. This small amount of product was always formed, irrespective of reaction conditions. B−H substitution in **1a**,**b** does not proceed further than this, even on heating, and we suggest that this is due to the coordination of the vinyl group to the rhodium metal center, which inhibits further substitution. The small amount of the bis-substituted cage presumably arises from reductive elimination of ethylcarborane from **B** (Scheme 3), which is in competition with β-elimination. This would lead to a small amount of ethyl-substituted cage that then undergoes a further dehydrogenative borylation. Consistent with this mechanism, there is a very small amount of the tris-substituted product also observed in the ESI-MS spectrum.

Intentional addition of H_2 to CH_2Cl_2 solutions of **1** results in rapid hydrogenation of the vinyl group, mediated by the rhodium

(39) Brown, J. M.; Lloyd-Jones, G. C. *J. Am. Chem. Soc.* **1994**, *116*, 866−878.
(40) Coapes, R. B.; Souza, F. E. S.; Thomas, R. L.; Hall, J. J.; Marder, T. B. *Chem. Commun.* **2003**, 614−615 and references cited therein.
(41) McKee, M. L. *J. Am. Chem. Soc.* **1997**, *119*, 4220−4223.
(42) Zakharkin, L. I.; Kovredov, A. I.; Ol'shevskaya, V. A. *Izv. Akad. Nauk SSSR, Ser. Khim.* **1985**, 888−92.
(43) Kalinin, V. N.; Kobel'kova, N. I.; Zakharkin, L. I. *Zh. Obshch. Khim.* **1977**, *47*, 963.
(44) Russell, J. M.; Sabat, M.; Grimes, R. N. *Organometallics* **2002**, *21*, 4113−4128.

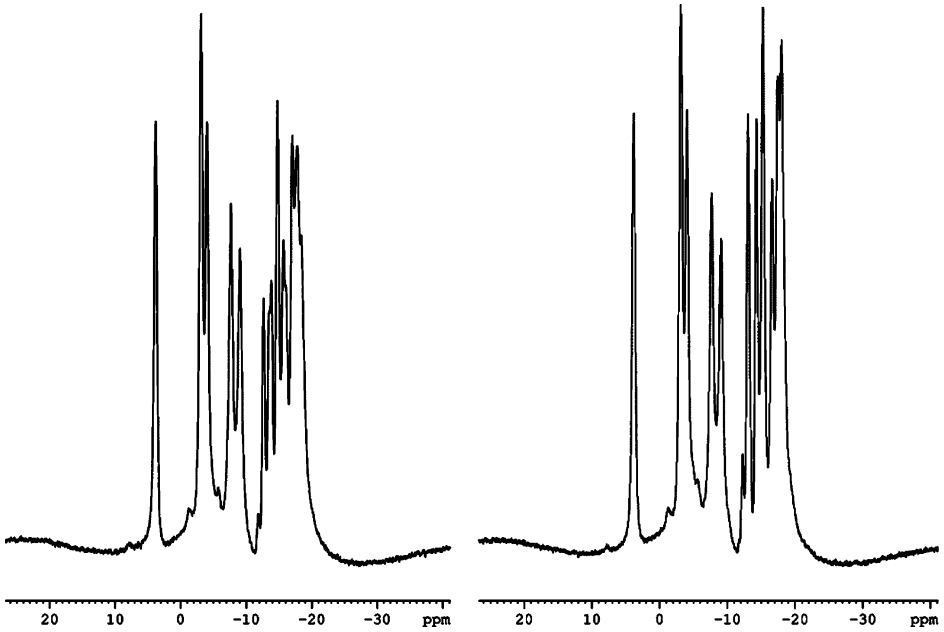

Figure 3. ^{11}B (left) and $^{11}B\{^1H\}$ (right) NMR spectra of **7** (160.46 MHz).

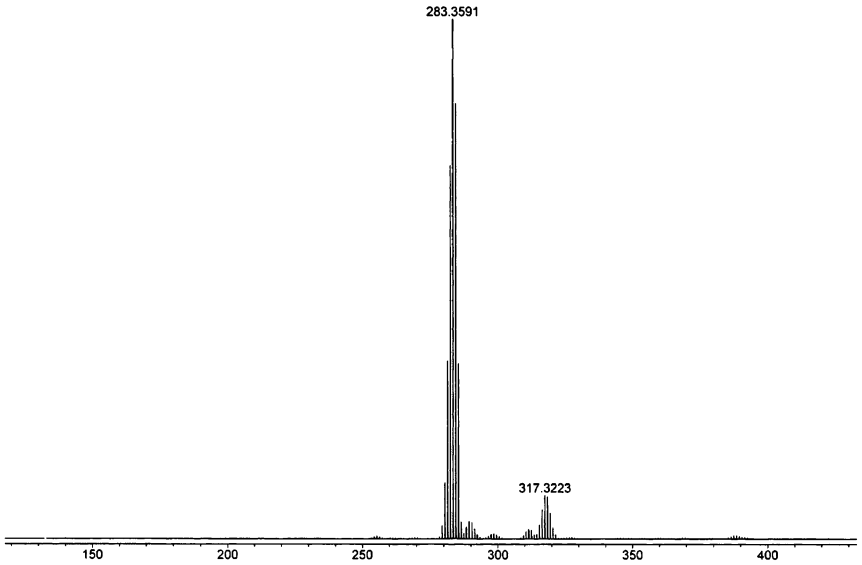

Figure 4. ESI-MS (negative mode) of **7**.

fragment,[35,45] to afford $Rh(PPh_3)_2$(1-H-12-(Et)-*closo*-$CB_{11}H_{10}$) (**3a**) and $Rh(PPh_3)_2$(1-H-7-(Et)-*closo*-$CB_{11}H_{10}$) (**3b**) (Scheme 4). A ^1H NMR spectrum of **3** shows the conversion of the vinyl group to ethyl, while the high-field region of the $^1H\{^{11}B\}$ NMR spectrum shows two broad signals attributed to the B−*H*−Rh bonds in either isomer, which broaden considerably in the ^1H NMR spectrum into poorly resolved quartets. Addition of nbd forms the salt $[Rh(PPh_3)_2(nbd)]$[1-H-7/12-(Et)-*closo*-$CB_{11}H_{10}$] (**4a**,**b**), which can be crystallized as an inseparable mixture of isomers. The ratio of 7- and 12-isomers remains the same throughout these transformations. On addition of nbd the high-field resonances due to Rh−*H*−B interactions in the ^1H NMR spectrum disappear.

Blocking the 12-position in the carborane cage with a bromine results in a single product. Addition of ethene to $Rh(PPh_3)_2$(1-H-12-Br-*closo*-$CB_{11}H_{10}$) gives the exclusive formation of $Rh(PPh_3)_2$(1-H-7-(CH_2═CH)-12-Br-*closo*-$CB_{11}H_9$) (**5**), which was

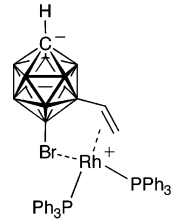

5

characterized by NMR spectroscopy. The ^1H NMR spectrum of **5** displays no low-frequency shifts that are indicative of Rh−*H*−B interactions, while the vinyl protons are observed between δ 5.03 and 3.81, suggestive of coordination to the $\{Rh(PPh_3)_2\}^+$ fragment, as when nbd is added to **5**, to produce $[Rh(PPh_3)_2$(nbd)][1-H-7-(CH_2═CH)-12-Br-*closo*-$CB_{11}H_9$] (**6**), these vinyl signals now shift downfield by over 1 ppm. These observations

(45) Behnken, P. E.; Busby, D. C.; Delaney, M. S.; King, R. E.; Kreimendahl, C. W.; Marder, T. B.; Wilczynski, J. J.; Hawthorne, M. F. *J. Am. Chem. Soc.* **1984**, *106*, 7444−7450.

Table 1. X-ray Crystallographic Data Collection and Refinement Details

	2a	**7**	**9**	**10**	**13**
formula	$C_{46}H_{52}B_{11}P_2Rh$	$C_{54}H_{70}B_{11}P_2Rh$	$C_{46}H_{59}B_{11}P_2RhSi$	$C_{44}H_{56}B_{11}P_2Rh$	$C_{47}H_{56}B_{11}Br_6Cl_8P_2Rh$
fw	888.64	1002.86	923.78	868.65	1667.74
cryst size, mm	0.55 × 0.55 × 0.30	0.20 × 0.10 × 0.05	0.25 × 0.13 × 0.08	0.20 × 0.13 × 0.03	0.50 × 0.25 × 0.20
T, K	150(2)	150(2)	150(2)	150(2)	150(2)
cryst syst	monoclinic	monoclinic	monoclinic	triclinic	triclinic
space group	$P2_1/c$	$P2_1/c$	$P2_1/a$	$P\bar{1}$	$P\bar{1}$
a, Å	17.0670(2)	16.7380(2)	18.8890(3)	9.8660(2)	11.3130(2)
b, Å	15.6010(2)	18.0910(2)	14.4860(3)	13.3420(4)	14.2250(2)
c, Å	17.4360(2)	18.5710(2)	20.2760(3)	17.7310(6)	22.6530(5)
α, deg	90	90	90	83.592(1)	96.597(1)
β, deg	101.895(1)	111.618(1)	116.272(1)	75.742(1)	92.376(1)
γ, deg	90	90	90	78.438(2)	112.9980(10)
V, Å^3	4542.86(9)	5227.88(10)	4974.94(15)	2211.41(11)	3318.63(10)
Z	4	4	4	2	2
μ, mm^{-1}	0.479	0.424	0.463	0.491	4.272
F_{000}	1832	2096	1916	900	1628
θ range, deg	3.58−28.70	3.45−27.49	5.54−25.00	5.57−27.44	3.64−27.51
D_{calcd}, g cm^{-3}	1.299	1.274	1.233	1.305	1.669
no. of collected/unique rflns	78 738/11 612	76 466/11 940	55 055/8611	26 014/9894	36 589/15 037
R1/wR2 ($I > 2\sigma(I)$)	0.0325/0.0798	0.0498/0.1095	0.0545/0.1017	0.0491/0.0905	0.049/0.136
R1/wR2 (all data)	0.0381/0.0854	0.0664/0.1173	0.0863/0.1209	0.0813/0.1028	0.0688/0.1352
GOF on F^2	1.050	1.052	1.108	1.034	1.04
max, min diff Fourier peaks, e Å^{-3}	0.680, −1.006	0.645, −0.476	0.951, −0.683	0.452, −0.678	1.49, −1.10

suggest a structure for **5** that has the metal phosphine fragment coordinated to the cage through a Rh−Br and a Rh−vinyl interaction. Monobrominated cages interacting with a metal fragment through the antipodal {BBr} vertex have been reported before.[46] Consistent with this structure that has inequivalent phosphines, the $^{31}P\{^1H\}$ NMR spectrum shows two broad environments at room temperature that sharpen into two well-resolved doublets of doublets at 258 K. There must be some fluxional process occurring to broaden the peaks at room temperature, and this might involve reversible breaking and making of the Rh−Br bond. The $^{11}B\{^1H\}$ NMR spectrum of **5** shows five broad environments, which resolve better in the nbd salt **6** to give a 1:1:2:2:2:2:1 pattern between δ −2.2 and −18.9 ppm, consistent with C_s symmetry. The first two signals are assigned by a combination of $^{11}B-^{11}B$ COSY and ^{11}B NMR spectroscopy as being due to BBr and *B*-vinyl groups, respectively. The nbd salt also shows only one environment in the $^{31}P\{^1H\}$ NMR spectrum, as expected.

Once the vinyl group has been hydrogenated in **3a**, the metal center becomes available to perform further dehydrogenative borylations. Addition of excess ethene to **3a** results in a mixture of products that can be identified by ESI-MS as resulting from two or three vertices being dehydrogenatively borylated. Addition of H_2 hydrogenates the vinyl groups to *B*-ethyls. Further cycling of ethene/H_2 addition four times (a total of six times in all) and addition of nbd results a compound that is identified by NMR spectroscopy, ESI-MS, and X-ray crystallography as $[Rh(PPh_3)_2(nbd)][1\text{-H-}2,4,8,10,12\text{-}(Et)_5\text{-}closo\text{-}CB_{11}H_6]$ (**7**; Scheme 5). This reaction affords product in ∼75% yield based on complex **I** and has been scaled to ∼1.5 g. The reaction mixture before addition of nbd shows broad, poorly resolved peaks in the ^{11}B NMR spectrum and evidence of Rh−H−B interactions in the high-field portion of the ^1H NMR spectrum (δ −4.95, br, B−*H*−Rh). Addition of a large excess of nbd to the reaction mixture results in decoordination of the cage from the carborane anion and a sharpening of the ^{11}B NMR spectrum, and for this reason full characterization has been carried out on this salt.

The solid-state structure of the anionic part of salt **7** is shown in Figure 2, and this shows fivefold substitution of the cage anion. There is some minor disorder associated with some of the ethyl groups, but this can be satisfactorily modeled. The cage carbon atom was identified on the basis of shorter C−B distances compared to distance for the other vertices. The substitution pattern is one in which the antipodal boron vertex, two lower pentagonal belt vertices, and two upper-belt vertices have been functionalized. No two adjacent vertices on the same pentagonal belt have been functionalized. This pattern presumably reflects that the sterically bulky $\{Rh(PPh_3)_2\}^+$ metal fragment sequentially inserts ethene into the B−H bonds which are least hindered and after five substitutions the resulting anion is too bulky to undergo further reaction. Although this results in no further substitutions, the benefit is that the metal fragment controls the substitution pattern and, thus, excellent regioselectivity is obtained. The B−C bonds in the cage (1.58(2)−1.630(7) Å) are similar to those found in the methylated carborane $[closo\text{-}CB_{11}Me_{12}]^-$ (1.59(2)−1.73(2) Å)[9] and the alkyl-substituted borane 6-$(CH_2{=}CHCH_2SiMe_2(CH_2)_3)$-*nido*-$B_{10}H_{13}$ (1.577(3) Å).[30]

The NMR spectra of **7** are consistent with the solid-state structure. In the ^1H NMR spectrum a broad (relative integral 25 H) set of signals is observed between δ 0.96 and 0.36 that is assigned to the ethyl groups. In the $^{11}B\{^1H\}$ NMR spectrum (160 MHz) nine resonances are observed in the ratio 1:1:1:1:1:1:1:1:1 (Figure 3) between δ 3.8 and −18.0. The first five of these signals (those most downfield) remain singlets in the ^{11}B NMR spectrum, identifying them as the B−Et vertices. ESI-MS of the reaction mixtures (Figure 4, *m*/*z* 283) demonstrates that fivefold substitution accounts for ∼95% of the products, with a very small amount of sixfold-substituted product also being observed (∼5%; see Figure 4). Analytically pure material can be obtained by repeated recrystallization. Multiple substitutions on polyborane cages using hydroboration methodology have been reported previously. $B_{10}H_{14}$ can be cleanly bisfunctionalized with alkenes by either $PtBr_2$ or stepwise incorporation using a $Cp_2Ti(CO)_2/PtBr_2$ combination.[28,30] Higher substitution products in the borylation of *arachno*-6,8-$C_2B_7H_{13}$ have been briefly mentioned but not characterized.[29] Up to three alkenyl groups can be incorporated in ruthenacarborane complexes by reactions with alkynes, affording B−H insertion products.[37] As far as we are aware, however, fivefold substitu-

(46) Patmore, N. J.; Ingleson, M. J.; Mahon, M. F.; Weller, A. S. *Dalton Trans.* **2003**, 2894−2904.

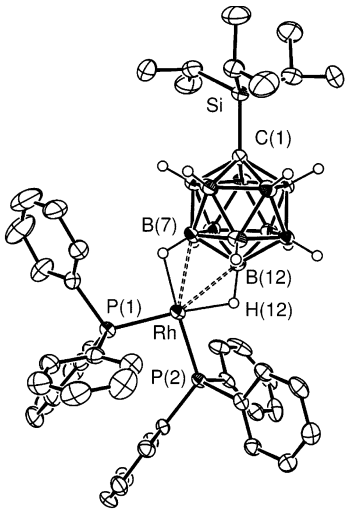

Figure 5. Solid-state structure of complex **9**. Thermal ellipsoids are shown at the 50% probability level. Hydrogen atoms, apart from those associated with cage vertices, have been omitted for clarity.

tion by hydroboration of a polyborane, as seen in **7**, has not been reported.

The degree of ethylation can be controlled by replacing the hydrogen on the cage carbon with a bulkier substituent. The rhodacarborane complexes $(PPh_3)_2Rh(1\text{-}R\text{-}closo\text{-}CB_{11}H_{11})$ have been prepared (R = Me (**8**), Si^iPr_3 (**9**)) by hydrogenation of the precursor complexes $[(PPh_3)_2Rh(nbd)][1\text{-}R\text{-}closo\text{-}CB_{11}H_{11}]$. Both complexes have been fully characterized by NMR spectroscopy and show the expected resonances due to Rh−H−B interactions in both the $^1H\{^{11}B\}$ and $^{11}B\{^1H\}$ NMR spectra.[35,38] The solid-state structure of **9** has also been determined (Figure 5), and this shows the $\{Rh(PPh_3)_2\}^+$ fragment to bind with the carborane cage with the antipodal (B12) and one lower pentagonal belt (B7) {BH} vertex, just as observed for the closely related complex **I**.[35]

Sequential addition of ethene/H_2 for three cycles to the methyl-substituted cage complex **8** afforded the new complex $Rh(PPh_3)_2(1\text{-Me-}9,11,12\text{-}(Et)_3\text{-}closo\text{-}CB_{11}H_8)$ (**10**), in which substitution has occurred in three places on the lower hemisphere of the cage, but the cage substituent has retarded further substitution on the upper-pentagonal belt of the anion (Scheme 6). Complex **10** has been characterized by NMR spectroscopy and ESI-MS. This latter technique shows the predominant product to be the triply substituted product, with a small amount (ca. 10%) of the doubly and quadruply substituted products also evident. Changing the reaction times, number of cycles, or temperature did not improve the ratio, and we could not isolate the material in bulk as a compositionally pure solid even after repeated crystallizations. Although the conversion was complete as measured by ^{11}B NMR spectroscopy, the isolated yields of impure solid **10** are low (25% based on Rh).

In the solid-state structure of **10** (Figure 6) the $\{Rh(PPh_3)_2\}^+$ fragment is coordinated through two Rh−H−B bonds on the lower pentagonal belt of the cage anion. B−H substitution has occurred in the antipodal and two separated lower belt {BH} vertices, a pattern that mirrors that observed in **7** for the same part of the cage. The labeled cage carbon vertex made the assignment of the substitution pattern unambiguous and also strengthens assignments made for the complexes which only had a {CH} vertex on the cage (e.g., **7**). The C−B distances in the substituted vertices fall into the same range as observed for **7** (1.590(6)−1.597(5) Å).

In solution, the Rh−H−B interactions are evidenced by a quadrupolar broadened integral 2H quartet at δ −4.64 ppm, while a broad (integral ∼15 H) signal between δ 1.02 and 0.11 ppm is observed for the B−Et groups. The ^{11}B NMR spectrum shows four resonances in the ratio 3:3:3:2, although some of these are overlapping resonances. The expected (for C_s symmetry) 1:2:1:2:2:1:2 pattern between δ −0.1 and −15.9 ppm is observed when excess nbd is added to afford $[Rh(PPh_3)_2(nbd)][1\text{-Me-}7,11,12\text{-}(Et)_3\text{-}closo\text{-}CB_{11}H_8]$ (**11**), in which the cage is no longer bound with the metal center (the Rh−*H*−B signals disappear). The two low-field resonances do not display coupling to ^1H in the ^{11}B NMR spectrum, identifying them as being due to *B*-Et vertices.

That the tris-substituted methylcarborane is not formed in compositionally pure form can be remedied by using the bulkier carbon substitutent Si^iPr_3. Cycling ethene/H_2 addition three times and then adding nbd affords $[Rh(PPh_3)_2(nbd)][1\text{-}(Si^iPr_3)\text{-}9,11,12\text{-}(Et)_3\text{-}closo\text{-}CB_{11}H_8]$ (**12**) as pure material in a reasonable yield (63%). Complex **12** has been characterized by NMR spectroscopy and ESI-MS. The $^{11}B\{^1H\}$ NMR spectrum of **12** (Figure 7) shows a pattern very similar to that of **11**, 1:2:1:2:2:3 between δ 7.7 and −16.8, again with the two lowest frequency peaks observed as singlets, showing that they can be assigned to *B*-Et vertices. Although the chemical shifts are not identical with those of **11**, they are similar enough to suggest that the substitution pattern is the same. The ESI-MS spectrum (Figure 8) shows one cage anion species with a mass and isotopic distribution appropriate for the composition (*m*/*z* 383). The bulkier Si^iPr_3 groups thus inhibit further substitution past three times better than the methyl group. Similarly, it has been briefly reported that incorporation of the silyl group in $[1\text{-}Si^iPr_3\text{-}closo\text{-}CB_{11}H_{11}]^-$ directs electrophilic methylation with MeOTf to occur only at the lower hemisphere of the cage.[11,12,47]

Attempts to make any of these transformations catalytic, for example using 20 mol % of **I** and $[1\text{-}Si^iPr_3\text{-}closo\text{-}CB_{11}H_{11}][NBu_4]$, did not lead to appreciable turnover, even though a variety of anion/metal fragment/solvent combinations were tried. Catalytic turnover has been observed in monohydroborations of *nido* cages using the $\{Rh(PPh_3)_2\}^+$ fragment and butyl acrylate.[32] The lack of reactivity in the systems under discussion here suggests that the cage anion is strongly bound to the metal fragment and cannot undergo ready exchange with the unsubstituted $[1\text{-H-}closo\text{-}CB_{11}H_{11}]^-$ cage. This is consistent with the dehydrogenative borylation process operating that results in a tightly bound vinylcarborane (e.g., **1a**,**b**). Hydrogenation of vinyl groups should remove this bottleneck, and indeed addition of $[NBu_4][1\text{-H-}closo\text{-}CB_{11}H_{11}]$ to **7** (the sterically most hindered carborane) results in partial exchange after 1 h to afford **I** and **7** in an approximate 1:4 ratio. However, the system is not catalytic in the sense that it does not turn over, as further addition of ethene results in the formation of vinylcarborane **1a**,**b**, which requires addition of H_2 to promote further B−H substitution. Attempts to generate metal-free salts using simple cations such as $[PPN]^+$ and $[NBu_4]^+$ also met with limited success, and we have not pursued this further.

Comments on the Mechanism of Borylation. The substitution pattern for dehydrogenative borylation follows from a simple charge distribution analysis in the $[1\text{-H-}closo\text{-}CB_{11}H_{11}]^-$ cage,[15,41] as well as the order of electrophilic substitution by either halogens[48] or DCl.[49] The electronegative cage carbon atom induces a dipole in the {BH} vertices in the cage that leads to the most negative boron vertices being BH(12)/BH(7-11). If it

(47) King, B. T. University of Colorado, Boulder, CO, 2000.
(48) Jelinek, T.; Plesek, J.; Hermanek, S.; Stibr, B. *Collect. Czech. Chem. Commun.* **1986**, *51*, 819−829.
(49) Jelinek, T.; Plesek, J.; Mares, F.; Hermanek, S.; Stibr, B. *Polyhedron* **1987**, *6*, 1981−1986.

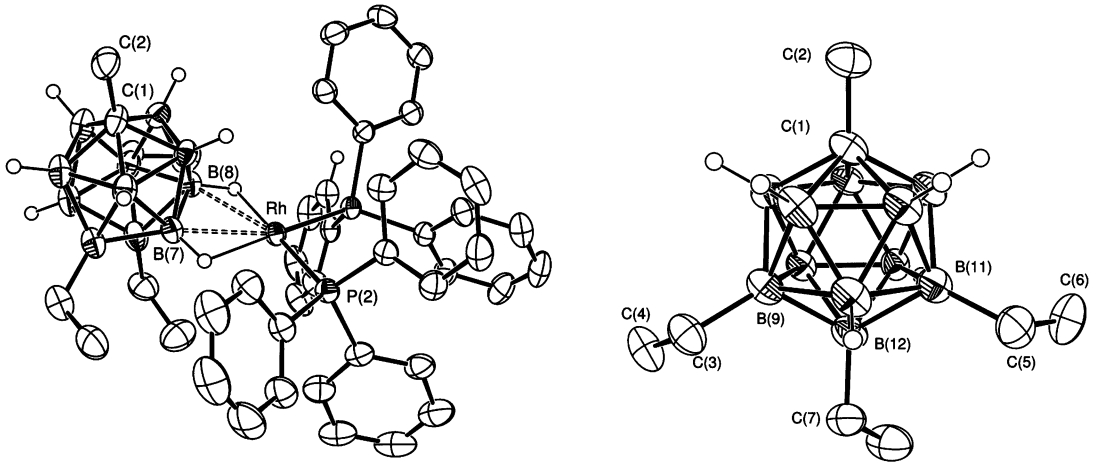

Figure 6. Solid-state structure of complex **10** (left) and of just the anion (right). Thermal ellipsoids are shown at the 50% probability level. Hydrogen atoms, apart from those associated with cage vertices, have been omitted for clarity.

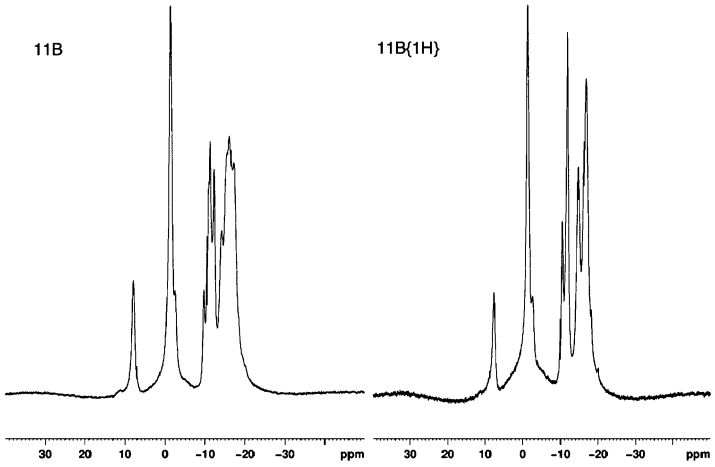

Figure 7. ^{11}B (left) and $^{11}B\{^1H\}$ (right) NMR spectra of **12**.

is assumed that the most electron rich {B−H} vertex undergoes preferential insertion with the $\{Rh(PPh_3)_2\}^+$ fragment in the absence of overriding steric effects, then the observed substitution pattern of B(12) → B(7-11) → B(2-5) is as expected when both electronic and steric factors are considered. Hydroboration using the carborane [7,8-$(CH_2)_3$-*nido*-$C_2B_9H_{10}]^-$ also occurs at the {BH} vertex farthest away from the cage carbon atoms.[32]

Exposure of $Rh(PPh_3)_2$(1-R-*closo*-$CB_{11}H_{11}$) (R = H, Me, Si^{i}Pr$_3$) to a D_2 atmosphere (1 atm) results in gradual (2 days) H/D exchange of all the {BH} vertices, as followed by ^{11}B and $^1H\{^{11}B\}$ NMR spectroscopy. The order of substitution, as determined from the $^1H\{^{11}B\}$ NMR spectrum, is as expected: B(12) followed by B(7-11) and finally B(2-5). The cage {CH} vertex is not deuterated. During this H/D exchange significant amounts of dissolved HD(g) were also observed (1:1:1 triplet at δ 4.55, J(DH) = 43 Hz), suggesting a mechanism for H/D exchange that involves an accessible dihydrogen/boryl intermediate such as **D** (Scheme 7). This is closely related to intermediate **A** in

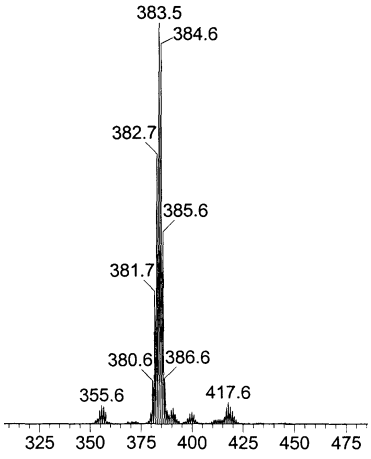

Figure 8. ESI-MS (negative mode) of **12**.

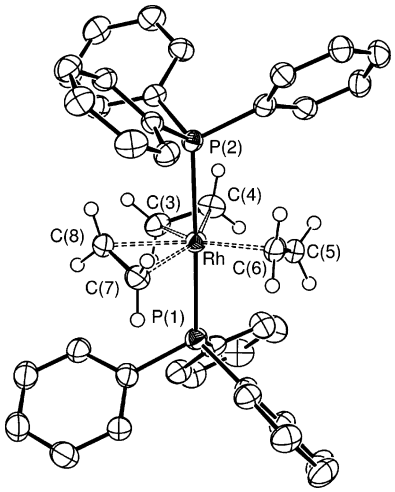

Figure 9. Solid-state structure of the cationic portion of complex **13**. Thermal ellipsoids are shown at the 50% probability level. Hydrogen atoms, apart from the olefin hydrogens, have been omitted for clarity.

Scheme 6

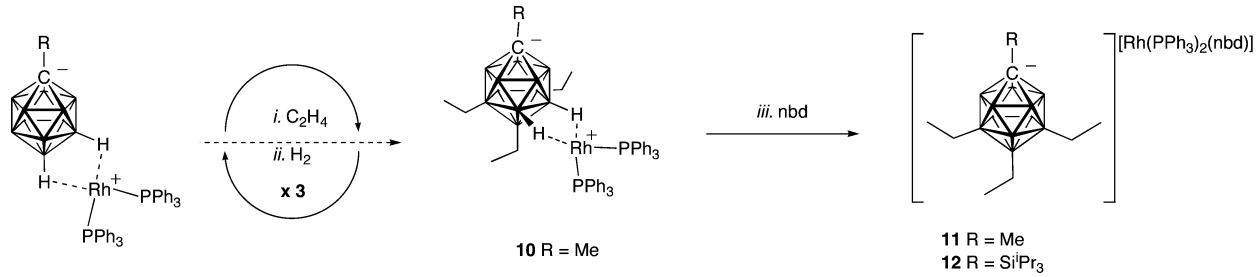

Scheme 7

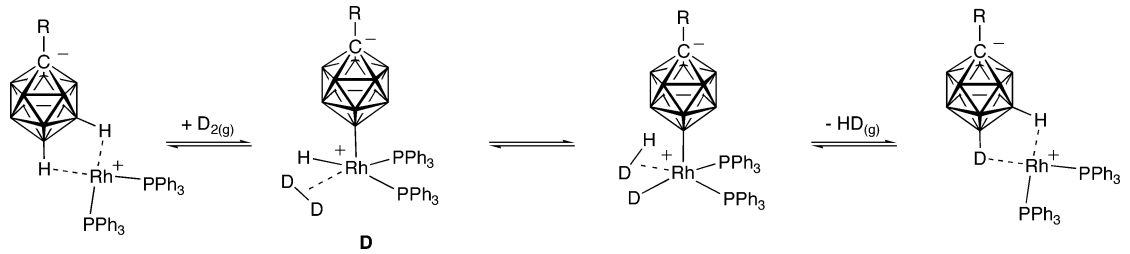

Scheme 8

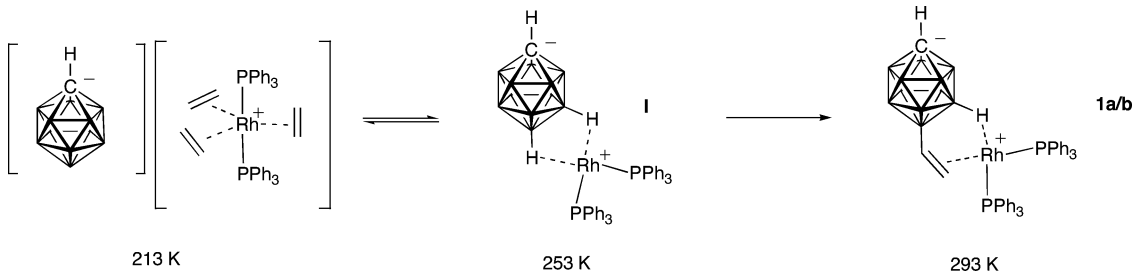

Scheme 3. Similar mechanisms, involving metal−boryl intermediates, have been proposed for the *exo-nido* complexes Rh(PPh$_3$)$_2$(7,8-R$_2$-*nido*-C$_2$B$_9$H$_{10}$).[45,50]

H/D exchange of every {BH} vertex also occurs in the ethyl-substituted complexes, even though no further dehydrogenative borylation occurs. For example, exposing **7** to a D_2 atmosphere for 2 days results in the complete replacement of the remaining {BH} vertices for {BD}, as measured by ^{1}H{^{11}B} and ^{11}B NMR spectroscopy and ESI-MS. This complete substitution suggests that the metal fragment is still able to insert into sterically protected {BH} vertices to generate intermediate boryl species but is not capable of further reaction with ethene. We suggest that it is the coordination of ethene and/or migratory insertion into the Rh−boryl bond which is disfavored with increasing cage substitution.

In an attempt to observe these putative Rh−boryl intermediates, reaction between **I** and excess ethene was monitored between 200 K and room temperature by ^{31}P{^{1}H} and ^{11}B{^{1}H} NMR spectroscopy. Between 200 and 230 K one species is observed in the ^{31}P{^{1}H} NMR spectrum, as a doublet at δ 35.5 (J(RhP) = 93 Hz). The ^{11}B{^{1}H} NMR spectrum shows no high-frequency peaks that would be indicative of direct metal boryl interactions,[51,52] while the distinctive 1:5:5 pattern for free [1-H-*closo*-CB$_{11}$H$_{11}$]$^-$ anion is observed at chemical shifts very close to those reported for the [NBu$_4$]$^+$ salt.[53] This suggests that the carborane cage is not interacting with the metal center. Confirming this, when the anion is changed to the weakly coordinating anions [BAr$^F_4$]$^-$ and [*closo*-CB$_{11}$H$_6$Br$_6$]$^-$ (by adding ethene to the aryl-bridged species [Rh(PPh$_3$){(η^6-C$_6$H$_5$)PPh$_2$}]$_2$[BAr$^F_4$]$_2$ or [Rh(PPh$_3$){(η^6-C$_6$H$_5$)PPh$_2$}]$_2$[1-*closo*-CB$_{11}$H$_6$Br$_6$]$_2$[35]), the ^{31}P{^{1}H} NMR spectrum remains the same. This complex has been characterized as the tris(ethene) species [Rh(PPh$_3$)$_2$(η^2-C$_2$H$_4$)$_3$][1-H-*closo*-CB$_{11}$H$_{11}$]. When the temperature is raised, signals due to **I** become increasingly intense at the expense of [Rh(PPh$_3$)$_2$(η^2-C$_2$H$_4$)$_3$][1-H-*closo*-CB$_{11}$H$_{11}$], and at 273 K **I** is the major species (Scheme 8). Cooling again establishes the same low-temperature spectrum, suggesting a dynamic equilibrium. When the temperature is raised to room temperature, dehydrogenative borylation commences, and signals due to **1a**,**b** are observed.

A crystal structure of the [*closo*-CB$_{11}$H$_6$Br$_6$]$^-$ salt unambiguously characterizes the low-temperature complex as the tris(ethene) species [Rh(PPh$_3$)$_2$(η^2-C$_2$H$_4$)$_3$][*closo*-CB$_{11}$H$_6$Br$_6$] (**13**). As **13** rapidly loses olefin when removed from an ethene atmosphere and also starts to lose ethene above −20 °C in solution, the crystals were grown from a cooled solution at −78 °C under an ethene atmosphere and mounted quickly on a precooled diffractometer. The solid-state structure is shown in Figure 9. Complex **13** shows a trigonal-bipyramidal structure in which the ethene ligands are arranged equatorially, adopting a geometry as expected from steric and electronic arguments.[54]

(50) Behnken, P. E.; Belmont, J. A.; Busby, D. C.; Delnay, M. S.; King, R. E.; Kreimendahl, C. W.; Marder, T. B.; Wilczynski, J. J.; Hawthorne, M. F. *J. Am. Chem. Soc.* **1984**, *106*, 3011−3025.

(51) Rath, N. P.; Fehlner, T. P. *J. Am. Chem. Soc.* **1987**, *109*, 5273−5274.

(52) Aldridge, S.; Coombs, D. L. *Coord. Chem. Rev.* **2004**, *248*, 535−559.

(53) Fox, M. A.; Mahon, M. F.; Patmore, N. J.; Weller, A. S. *Inorg. Chem.* **2002**, *41*, 4567−4573.

(54) Albright, T. A.; Burdett, J. K.; Whangbo, M.-H. *Orbital Interactions in Chemistry*; Wiley: New York, 1985.

The structure is very similar to the structure we have reported for $[Ir(PPh_3)_2(\eta^2\text{-}C_2H_4)_3][closo\text{-}CB_{11}H_6Br_6]$[55] and is also similar to that of the acetonitrile complex $[Rh(NCMe)_2(\eta^2\text{-}C_2H_4)_3][BF_4]$.[56] The analogous complex $[Rh(PMe_3)_2(\eta^2\text{-}C_2H_4)_3][PF_6]$ has been spectroscopically characterized in solution.[57] The Rh−C_{ethene} distances and C−C distances for **13** are as expected (2.246(4)−2.287(4) and 1.362(7)−1.375(7) Å, respectively) for a cationic metal center with three π-accepting ligands with little Rh→C back-donation (free ethene d(CC) = 1.337 Å). The analogous complex $[Ir(PPh_3)_2(\eta^2\text{-}C_2H_4)_3][closo\text{-}CB_{11}H_6Br_6]$ is significantly more stable than **13** toward ethene loss,[55] a consequence of the stronger Ir−C bonds. Replacement of weakly bound carboranes via other ligands has been reported before. For example, $Rh(PPh_3)_2(7,8\text{-}R_2\text{-}nido\text{-}C_2B_9H_{10})$ reacts with CO to afford $[Rh(PPh_3)_2(CO)_3][7,8\text{-}R_2\text{-}nido\text{-}C_2B_9H_{10}]$, in which the cation is directly related to **13** (R = alkyl, Ph).[58]

Conclusions

Ethylation of $[1\text{-}H\text{-}closo\text{-}CB_{11}H_{11}]^-$ by a rhodium phosphine mediated route has been shown to be effective for the introduction of up to five ethyl groups on the cage through sequential dehydrogenative borylation/hydrogenation of ethene. Although this accesses new substitution patterns, per-boron-vertex substitution using this route was not achieved, due to the increasingly bulky ethyl-substituted carborane becoming reluctant to undergo further borylation with ethene. Unfortunately, the fact that the functionalized cage is difficult to produce in pure form without an associated metal fragment and that the overall process does not turnover in a catalytic sense means that this methodology is somewhat limited for producing functionalized carborane cage anions. Studies to improve both the scope and possibility of catalytic turnover in this process are underway.

Experimental Section

General Considerations. All manipulations were carried out under an atmosphere of argon, using standard Schlenk-line and glovebox techniques, unless otherwise stated. Glassware was predried in an oven at 130 °C and flamed with a blowtorch under vacuum prior to use. Solvents were dried over activated alumina, copper, and molecular sieve columns using an MBraun solvent purification system. CD_2Cl_2 was distilled under vacuum from CaH_2. $(PPh_3)_2Rh(1\text{-}H\text{-}closo\text{-}CB_{11}H_{11})$ and $(PPh_3)_2Rh(1\text{-}Me\text{-}closo\text{-}CB_{11}H_{11})$ (**8**) were prepared by the published literature routes or slight variations thereof.[35,38] $[(PPh_3)_2Rh(nbd)][1\text{-}^iPr_3Si\text{-}closo\text{-}CB_{11}H_{11}]$ and $(PPh_3)_2Rh(1\text{-}H\text{-}12\text{-}Br\text{-}closo\text{-}CB_{11}H_{10})$ were prepared as outlined in the Supporting Information. All other chemicals were used as received from Aldrich. Microanalyses were performed by Elemental Microanalysis Limited. Mass spectrometry was performed by the EPSRC Service at the University of Swansea or at the University of Bath using a Bruker MicroToF mass spectrometer equipped with an electrospray ionization source.

NMR Spectroscopy. ^1H, $^1H\{^{11}B\}$, $^{11}B\{^1H\}$, ^{11}B, and $^{31}P\{^1H\}$ NMR spectra were recorded on Brüker Avance 300, 400, and 500 MHz spectrometers. Residual protio solvent was used as reference for ^1H and $^1H\{^{11}B\}$ NMR spectra (CD_2Cl_2, δ = 5.33). ^{11}B and $^{11}B\{^1H\}$ and $^{31}P\{^1H\}$ spectra were referenced against $BF_3{\cdot}OEt_2$ (external) and 85% H_3PO_4 (external), respectively. Values are quoted in ppm. Coupling constants are quoted in Hz.

X-ray Crystallography. Intensity data for all structures were collected at 150 K on a Nonius KappaCCD diffractometer equipped with a low-temperature device, using graphite-monochromated Mo Kα radiation (λ = 0.710 73 Å). Data were processed using the Nonius software.[59] For **13** a symmetry-related (multiscan) absorption correction was applied. Crystal parameters and details on the data collection, solution, and refinement for the complexes are provided in Table 1. Structure solution, followed by full-matrix least-squares refinement, was performed using the WINGX-1.70 suite of programs throughout.[60] The crystal data are available from the Cambridge Crystallographic Database: CCDC reference numbers 268853 (**10**), 268854 (**7**), 632281 (**2a**), 632282 (**9**), and 632283 (**13**). For **9** and **10** the bridging Rh−*H*−B hydrogen atoms were located in the difference Fourier map and freely refined. For **7** one phenyl ring of the PPh_3 ligand showed rotational disorder in the ratio of 85:15. Three out of the five ethyl group substituents of the anion borane cage were refined with site occupation of 60:40, and due to partial overlap of the ellipsoids the disordered atom pair C54/C54A was refined isotropically. Complex **13** crystallizes with four molecules of CH_2Cl_2 spread over six sites. The CH_2Cl_2 pair of C81/C81A was refined in a ratio of 90:10 with the minor C atom refined isotropically, and the pair C84/C85 showed a site occupancy of 1:1. Cl9 in the CH_2Cl_2 molecule associated with C85 was disordered in the ratio 1:1. The CH_2Cl_2 atoms C82 and C83 were fully occupied, but one of the Cl atoms in each molecule showed disorder in the ratios of 1:1 (Cl4/Cl4A) and 3:2 (Cl5/Cl5A). Most C−Cl bond lengths were idealized. Vinyl hydrogen atoms were located in the difference Fourier map and freely refined. Full bond lengths and angles are provided in the Supporting Information.

$Rh(PPh_3)_2(1\text{-}H\text{-}7/12\text{-}(CH{=}CH_2)\text{-}closo\text{-}CB_{11}H_{10})$ (12-Isomer (1a), 7-Isomer (1b)). $(PPh_3)_2Rh(1\text{-}H\text{-}closo\text{-}CB_{11}H_{11})$ (45 mg, 0.058 mmol) was placed in a 15 cm^3 Young ampule, and CH_2Cl_2 (5 cm^3) was added via cannula. The solution was freeze−pump−thawed three times. On the third cycle the solution was charged with ethene (0.500 g) the ampule was closed, and the mixture was warmed to room temperature with stirring. After 15 h, the solvent was evaporated under vacuum and the residue washed with pentane and dried to afford a dark orange product (28 mg, 61%). Anal. Calcd for $C_{39}H_{44}B_{11}P_2Rh$: C, 58.81; H, 5.57. Found: C, 58.57; H, 5.57.

^1H NMR (δ, CD_2Cl_2): 7.81−7.06 (m, 30H, PPh_3), 4.95 (d, 1H, B−CH=CH_2, J(HH) = 9, 7-isomer), 4.83 (d, 1H, B−CH=CH_2, J(HH) = 16, 12-isomer), 4.15 (d, 1H, B−CH=CH_2, J(HH) = 9, 7 isomer), 4.10 (d, 1H, B−CH=CH_2, J(HH) = 9, 12-isomer), 2.67 (dd, 1H, B−C*H*=CH_2, J(HH) = 16, ^3J(HH) = 9, 7-isomer), 2.56 (dd, 1H, B−C*H*=CH_2, J(HH) = 16, J(HH) = 9, 12-isomer), 2.37 (s, 1H, C_{cage}−*H*, 7-isomer), 2.22 (s, 1H, C_{cage}−*H*, 12-isomer). Selected $^1H\{^{11}B\}$ NMR (δ, CD_2Cl_2): 1.86 (br s, B−*H*, 7-isomer), 1.80 (br s, B−*H*, 7-isomer), 1.64 (br s, B−*H*, 7-isomer), 1.52 (br, B−*H*, 12-isomer), 1.24 (br s, B−*H*, 7-isomer), 0.18 (br s, B−*H*, 7-isomer), −0.56 (br, B−*H*, 12-isomer), −0.80 (br s, B−*H*−Rh, 7-isomer), −1.72 (br, B−*H*−Rh, 12-isomer), −2.15 (br s, B−*H*−Rh, 7-isomer). ^{11}B NMR (δ CD_2Cl_2): 2.71 (s, *B*−C), −2.18 (s, *B*−C), −14.93 (br, overlapping signals). $^{31}P\{^1H\}$ NMR (δ, CD_2Cl_2, 298 K): 40.7 (br).

$[Rh(PPh_3)_2(nbd)][1\text{-}H\text{-}7/12\text{-}(CH{=}CH_2)\text{-}closo\text{-}CB_{11}H_{10}]$ (12-Isomer (2a), 7-Isomer (2b)). Norbornadiene (100 equiv) was added to a CH_2Cl_2 solution of **1a**,**b** as described above, and the mixture was stirred for 3 h. The solvent was evaporated under vacuum and the residue redissolved in CH_2Cl_2 (2 cm^3) and precipitated with pentane (15 cm^3) to afford an orange precipitate. The solvent was decanted via cannula and the product (44 mg, 85%) dried under vacuum. ESI-MS (negative mode): *m*/*z* 169.2, showing the correct

(55) Rifat, A.; Kociok-Kohn, G.; Steed, J. W.; Weller, A. S. *Organometallics* **2004**, *23*, 428−432.
(56) Maspero, F.; Perrotti, E.; Simonetti, F. *J. Organomet. Chem.* **1972**, *38*, C43−C45.
(57) Werner, H.; Feser, R. *Z. Naturforsch., B: Anorg. Chem. Org. Chem.* **1980**, *35B*, 689−693.
(58) Long, J. A.; Marder, T. B.; Behnken, P. E.; Hawthorne, M. F. *J. Am. Chem. Soc.* **1984**, *106*, 2979−2989.
(59) Otwinowski, Z.; Minor, W. In *Methods Enzymol.* **1997**, *276*.
(60) Farrugia, L. J. *J. Appl. Crystallogr.* **1999**, *32*, 837−838.

isotope pattern for $B_{11}C_3H_{14}$. Anal. Calcd for $C_{46}H_{52}B_{11}P_2Rh$: C, 62.17; H, 5.90. Found: C, 61.75; H, 6.08.

^{1}H NMR (δ, CD_2Cl_2): 7.50−7.26 (m, 30H, PPh_3), 6.35 (dd, BC*H*=CH_2, *J*(HH) = 19, *J*(HH) = 13, 7-isomer), 6.23 (dd, B−C*H*=CH_2, *J*(HH) = 19, *J*(HH) = 13, 12-isomer), 5.53 (br s, B−CH=C*H*$_2$, 7-isomer), 5.35 (br s, B−CH=C*H*$_2$, 7- and 12-isomers), 5.18 (br s, B−CH=C*H*$_2$, 12-isomer), 4.50 (br s, 4H, C_7H_8), 4.08 (br s, 2H, C_7H_8), 2.44 (br s, C_{cage}−*H*, 7-isomer), 2.31 (br s, 1H, C_{cage}−*H*, 12-isomer), 1.56 (s, 2H, C_7H_8). ^{11}B{^{1}H} NMR (δ, CD_2Cl_2; assignments from ^{11}B−^{11}B COSY and ^{11}B NMR, primed numbers indicate 7-isomer): 1.2 (*B12*−CH=CH_2), −4.6 (*B7′*−CH=CH_2), −5.8 (*B12′*−H), −12.4 (*B7*−*11*,*8′*,*11′*−H, coincident signal), −13.4 (*B9′*,*10′*−H), −15.6 (*B2′*,*3′*−H), −16.4 (*B2*−*6*,*4′*,*6′*-H, coincident signal), −18.5 (*B5′*−H). ^{31}P{^{1}H} NMR (δ, CD_2Cl_2, 298 K): 29.6 (d, *J*(RhP) = 156).

Rh(PPh$_3$)$_2$(1-H-7/12-(Et)-*closo*-CB$_{11}$H$_{10}$) (12-Isomer (3a), 7-Isomer (3b)). (PPh_3)$_2$Rh(1-H-*closo*-$CB_{11}H_{11}$) (45 mg, 0.058 mmol) was placed in a 15 cm^3 Young ampule, and CH_2Cl_2 (5 cm^3) was added via cannula. The solution was freeze−pump−thawed three times. On the third cycle the solution was charged with ethene (1.012 g) and warmed to room temperature with stirring. After 15 h, excess ethene was removed under vacuum and replaced with hydrogen (1 atm). After 1 h, the solvent was evaporated under vacuum to afford a red product (25 mg, 54%). Anal. Calcd for $C_{39}H_{46}B_{11}P_2Rh$: C, 58.66; H, 5.81. Found: C, 58.04; H, 5.85.

^{1}H NMR (δ CD_2Cl_2): 7.80−7.06 (m, 30H, PPh_3), 2.51 (br s, 1H, C_{cage}−*H*, 12-isomer), 2.46 (s, 1H, C_{cage}−*H*, 7-isomer), 0.95−0.30 (m, B−*Et*), -0.84 (br q, B−*H*−Rh), −2.11 (br q, B−*H*−Rh). Selected ^{1}H{^{11}B} NMR (δ, CD_2Cl_2): 2.51 (br s, 1H, C_{cage}−*H*, 12-isomer), 2.46 (s, 1H, C_{cage}−*H*, 7-isomer), 1.98 (br s, B−*H*), 1.64 (br s, B−*H*), 1.55 (br s, B−*H*), 1.44 (br s, B−*H*), 0.95−0.30 (m, B−*Et*), −0.84 (br s, B−*H*−Rh), −2.11 (br s, B12−*H*−Rh). ^{11}B-{^{1}H} NMR (δ, CD_2Cl_2): 8.51 (s, *B*−H), 5.04 (s, *B*−H), 2.67 (s, *B*−H), 0.89 (s, *B*−H), −12.00 (s, *B*−H), −14.18 (s, *B*−H), −16.12 (s, *B*−H), −16.89 (s, *B*−H). ^{31}P{^{1}H} NMR (δ, CD_2Cl_2, 298 K): 12-isomer, 46.0 (d, *J*(RhP) = 194); 7-isomer, 45.8 (d, *J*(RhP) = 189).

[Rh(PPh$_3$)$_2$(nbd)][1-H-7/12-(Et)-*closo*-CB$_{11}$H$_{10}$] (12-Isomer (4a), 7-Isomer (4b)). (PPh_3)$_2$Rh(1-H-*closo*-$CB_{11}H_{11}$) (45 mg, 0.058 mmol) was placed in a 15 cm^3 Young ampule, and CH_2Cl_2 (5 cm^3) was added via cannula. The solution was freeze−pump−thawed three times. On the third cycle the solution was charged with ethene (1.012 g) and warmed to room temperature with stirring. After 15 h, excess ethene was removed under vacuum and replaced with hydrogen (1 atm). After 1 h, the solvent was evaporated under vacuum. The residue was redissolved in CH_2Cl_2, and norbornadiene (0.5 cm^3, 4.63 mmol) was added. After the mixture was stirred for 3 h, the solvent was evaporated under vacuum and the orange residue redissolved in CH_2Cl_2 (2 cm^3) and precipitated with pentane (15 cm^3). The solvent was decanted via cannula and the product (44 mg, 85%) dried under vacuum. ESI-MS (negative mode): *m*/*z* 171.1, showing the correct isotope pattern for $B_{11}C_3H_{16}$. Anal. Calcd for $C_{46}H_{54}B_{11}P_2Rh$: C, 62.03; H, 6.11. Found: C, 61.70; H, 6.22. ^{1}H NMR (δ, CD_2Cl_2): 7.37−7.27 (m, 30H, PPh_3), 4.47 (br s, 4H, C_7H_8), 3.99 (br s, 2H, C_7H_8), 2.26 (br s, C_{cage}−*H*), 2.16 (br s, C_{cage}−*H*), 1.59 (br s, 2H, C_7H_8), 1.06-0.70 (m, B−*Et*). ^{1}H{^{11}B} NMR (δ, CD_2Cl_2): 7.37−7.27 (m, 30H, PPh_3), 4.47 (br s, 4H, C_7H_8), 3.99 (br s, 2H, C_7H_8), 2.26 (br s, C_{cage}−*H*), 2.16 (br s, C_{cage}−*H*), 1.63 (br s, B−*H*), 1.61 (br s, B−*H*), 1.59 (br s, 2H, C_7H_8), 1.55 (br s, B−*H*), 1.06−0.70 (m, B−*Et*). ^{11}B NMR (δ, CD_2Cl_2; assignments from ^{11}B−^{11}B COSY, primed numbers indicate 7-isomer): 4.13 (s, *B12*−Et), -1.78 (s, *B7′*−Et), −6.20 (d, *B12′*−H, *J*(BH) = 133), −12.77 (d, *B7*−*11*,*8′*,*11′*−H, *J*(BH) = 136), −14.03 (d br, *B9′*,*10′*−H), −16.00 (d br, *B2′*,*3′*−H), −16.90 (d, *B2*−*6*,*4′*,*6′*−H, *J*(BH) = 147), −19.81 (d, *B5′*−H, *J*(BH) = 149). ^{31}P{^{1}H} NMR (δ, CD_2Cl_2, 298 K): 29.4 (d, *J*(RhP) = 155).

Rh(PPh$_3$)$_2${1-H-7-(CH=CH$_2$)-12-Br-*closo*-CB$_{11}$H$_9$} (5). [Rh(PPh$_3$)$_2$(nbd)][1-H-12-Br-*closo*-$CB_{11}H_{10}$] (50 mg, 0.053 mmol) was placed in a 15 cm^3 Young ampule equipped with a magnetic stirrer, and CH_2Cl_2 (5 cm^3) was added via cannula. The solution was freeze−pump−thawed three times. On the third cycle the solution was warmed to room temperature with stirring under an atmosphere of hydrogen to give [(PPh$_3$)$_2$Rh(1-H-12-Br-*closo*-$CB_{11}H_{11}$)] (see the Supporting Information for NMR data). After 30 min excess hydrogen was removed with vacuum and ethene was condensed in (1.407 g). After 24 h excess ethene was released, the solvent evaporated under vacuum, and the residue redissolved with CH_2Cl_2. The solution was concentrated under reduced pressure to a volume of 3 cm^3, and hexanes (20 cm^3) was added to afford an orange precipitate. Solvents were removed by decantation and the product was washed with hexane (2 × 5 cm^3) and dried in vacuo to afford the title compound (22 mg, 47%) as an orange solid. Anal. Calcd for $C_{39}H_{43}B_{11}BrP_2Rh(CH_2Cl_2)_2$: C, 47.11; H, 4.53. Found: C, 47.97; H, 4.83.

^{1}H NMR (δ, CD_2Cl_2, 298 K): 7.44−7.14 (m, 30H, PPh_3), 5.03 (d, 1H, B−CH=C*H*$_2$, *J*(HH) = 16), 4.45 (d, 1H, B−CH=C*H*$_2$, *J*(HH) = 9.6), 3.18 (dd, 1H, B−C*H*=CH_2, *J*(HH) = 16, *J*(HH) = 9.6), 2.26 (s, 1H, C_{cage}−*H*). Selected ^{1}H{^{11}B} NMR (δ, CD_2Cl_2 298 K): 1.74 (br s, B−*H*), 1.60 (br s, B−*H*). ^{11}B{^{1}H} NMR (δ, CD_2Cl_2, 298 K): −2.35 (s, *B*−C), -3.64 (s, *B*−Br), -12.80 (br s, *B*−H), −14.33 (br s, *B*−H), −17.07 (br s, *B*−H). ^{31}P{^{1}H} NMR (δ, CD_2Cl_2, 298 K): 57.4 (br s), 21.4 (br s). ^{31}P{^{1}H} NMR (δ, CD_2Cl_2, 258 K): 57.4 (dd, *J*(RhP) = 194, *J*(PP) = 32), 21.4 (dd, *J*(RhP) = 194, *J*(PP) = 32).

[Rh(PPh$_3$)$_2$(nbd)][1-H-7-(CH=CH$_2$)-12-Br-*closo*-CB$_{11}$H$_9$] (6). [Rh(PPh$_3$)$_2$(nbd)][1-H-12-Br-*closo*-$CB_{11}H_{10}$] (100 mg, 0.106 mmol) was placed in a 15 cm^3 Young ampule equipped with a magnetic stirrer, and CH_2Cl_2 (5 cm^3) was added via cannula. The solution was freeze−pump−thawed three times. On the third cycle the solution was warmed to room temperature with stirring under an atmosphere of hydrogen to give [(PPh$_3$)$_2$Rh(12-Br-$CB_{11}H_{11}$)]. After 30 min excess hydrogen was removed with vacuum and ethene condensed (1.542 g). After 2 h, ethene was released, the solvent evaporated under vacuum, and the residue redissolved with CH_2Cl_2. Norbornadiene (0.5 cm^3, 4.63 mmol) was added to the CH_2Cl_2 solution and stirred for 3 h. The solvent was evaporated under vacuum and the residue redissolved in CH_2Cl_2 (2 cm^3) and precipitated with pentane (15 cm^3) to afford an orange precipitate. Solvents were removed by decantation, and the product was washed with pentane (2 × 5 cm^3) and dried in vacuo to afford the title compound (85 mg, 83%) as an orange solid. ESI-MS (negative mode), *m*/*z* 248.2, showing the correct isotope pattern for $C_3H_{13}B_{11}$-Br. Anal. Calcd for $C_{46}H_{51}B_{11}BrP_2Rh$: C, 57.10; H, 5.31. Found: C, 57.16; H, 5.33.

^{1}H NMR (δ, $CDCl_3$): 7.40−7.27 (m, 30H, PPh_3), 6.32 (dd, B−C*H*=CH_2, *J*(HH) = 19, *J*(HH) = 13), 5.61 (br s, 1H, B−CH=C*H*$_2$), 5.45 (br s, 1H, B−CH=C*H*$_2$), 4.50 (br s, 4H, C_7H_8), 4.08 (br s, 2H, C_7H_8), 2.40 (br s, C_{cage}−*H*), 1.57 (s, 2H, C_7H_8). ^{1}H{^{11}B} NMR (δ, $CDCl_3$): 7.40−7.27 (m, 30H, PPh_3), 6.32 (dd, B−C*H*=CH_2, *J*(HH) = 19, *J*(HH) = 13), 5.61 (dd, 1H, B−CH=C*H*$_2$, *J*(HH) = 19, *J*(HH) = 4.6), 5.45 (dd, 1H, B−CH=C*H*$_2$, *J*(HH) = 13, *J*(HH) = 4.6), 4.50 (br s, 4H, C_7H_8), 4.08 (br s, 2H, C_7H_8), 2.40 (br s, C_{cage}−*H*), 2.14 (br s, 2H, B−*H*), 2.07 (br s, 2H, B−*H*), 1.93 (br s, 2H, B−*H*), 1.81 (br s, 2H, B−*H*), 1.74 (br s, 1H, B−*H*), 1.57 (s, 2H, C_7H_8). ^{11}B{^{1}H} NMR (δ, $CDCl_3$; assignments from ^{11}B−^{11}B COSY and ^{11}B NMR): −2.16 (s, 1B, *B*−Br), −5.38 (s, 1B, *B*−C), −11.73 (s, 2B, *B*−H), −12.63 (s, 2B, *B*−H), −16.48 (s, 2B, *B*−H), −17.43 (s, 2B, *B*−H), −18.87 (s, 1B, *B*−H). ^{31}P-{^{1}H} NMR (δ, $CDCl_3$): 29.8 (d, *J*(RhP) = 156).

[Rh(PPh$_3$)$_2$(nbd)][1-H-2,4,8,10,12-(Et)$_5$-*closo*-CB$_{11}$H$_6$] (7). A solution of (PPh_3)$_2$Rh(1-H-*closo*-$CB_{11}H_{11}$) (179 mg, 0.232 mmol) in CH_2Cl_2 (10 cm^3) was freeze−pump−thawed three times. On the third cycle ethene (∼0.600 g) was added to the solution and

the ampule closed and warmed to room temperature. After it was stirred for 24 h, the solution was degassed again, hydrogen was placed in the Young ampule, and the solution was stirred for 2 h. This sequential treatment with ethene/hydrogen was repeated a total of six times. Following the last hydrogenation the solvent was degassed and norbornadiene (1 cm^3, 9.27 mmol) added. After the mixture was stirred overnight, the solvent was evaporated under vacuum and the orange residue redissolved in CH_2Cl_2 (2 cm^3) and precipitated with hexane (20 cm^3). The solvent was decanted via cannula and the product (175 mg, 75%) dried under vacuum. Crystals suitable for an X-ray diffraction study were grown from CH_2Cl_2/pentane solutions. Anal. Calcd for $RhP_2B_{11}C_{54}H_{70}$: C, 64.67; H, 7.04. Found: C, 64.50; H, 7.23. ESI-MS (negative mode): *m*/*z* 283.3. This preparation has been successfully scaled up to 1.5 g of material with only a small overall loss in yield (∼70%).

^{1}H NMR (δ, CD_2Cl_2): 7.49−7.20 (m, 30H, PPh_3), 4.44 (br s, 4H, C_7H_8), 3.96 (br s, 2H, C_7H_8), 2.02 (br s, C_{cage}−*H*), 1.55 (br s, 2H, C_7H_8), 0.96−0.36 (m, 25H, B−*Et*). ^{1}H{^{11}B} NMR (δ, CD_2Cl_2): 7.49−7.20 (m, 30H, PPh_3), 4.44 (br s, 4H, C_7H_8), 3.96 (br s, 2H, C_7H_8), 2.02 (br s, C_{cage}−*H*), 1.55 (br s, 2H, C_7H_8), 1.48 (br s, B−*H*), 1.40 (br s, B−*H*), 1.36 (br s, B−*H*), 1.29 (br s, B−*H*), 1.21 (br s, B−*H*), 1.08 (br s, B−*H*), 0.96-0.36 (m, 25H, B−*Et*). ^{11}B-{^{1}H} NMR (δ, CD_2Cl_2): 3.8 (br s, 1B, *B*−Et), −3.2 (br s, 1B, *B*−Et), −4.0 (br s, 1B, *B*−Et), −8.0 (br s, 1B, *B*−Et), −9.0 (br s, 1B, *B*−Et), -13.0 (br s, 1B, *B*−Et) −14.3 (br s, 1B, *B*−H), −15.2 (br s, 1B, *B*−H), −16.6 (br s, 1B, *B*−H), −17.4 (br s, 1B, *B*−H), −18.0 (br s, 1B, *B*−H). ^{31}P{^{1}H} NMR (δ, CD_2Cl_2, 298 K): 30.5 (d, *J*(RhP) = 155).

(PPh_3)$_2$Rh(1-^{i}Pr$_3$Si-*closo*-$CB_{11}H_{11}$) (9). [(PPh_3)$_2$Rh(nbd)][1-^{i}Pr$_3$-Si-*closo*-$CB_{11}H_{11}$] (30 mg, 0.029 mmol) was placed in a 15 cm^3 Young ampule, and CH_2Cl_2 (5 cm^3) was added via cannula. The solution was freeze−pump−thawed three times. On the third cycle the solution was warmed to room temperature with stirring, under an atmosphere of H_2. Conversion was quantitative by NMR spectroscopy. Addition of hexanes along with solvent evaporation under vacuum afforded a dark red product. Suitable crystals for X-ray diffraction studies were obtained from a concentrated CH_2Cl_2 solution at −18 °C. Anal. Calcd for $C_{46}H_{62}P_2RhSiB_{11}$: C, 59.61; H, 6.74. Found: C, 60.3; H, 6.54.

^{1}H NMR (δ, $CDCl_3$): 7.51−7.07 (m, 30H, PPh_3), 1.18 (sept, 3H, Si(C*H*(CH$_3$)$_2$)$_3$), 1.11 (d, 18H, Si(CH(C*H*$_3$)$_2$)$_3$), 0.07 (br q, 5H, B(7−11)−*H*), −0.08 (br q, 1H, B(12)−*H*). ^{1}H{^{11}B} NMR (δ, $CDCl_3$): 7.51−7.07 (m, 30H, PPh_3), 2.05 (s, 5H, B(2−6)−*H*), 1.18 (sept, 3H, Si(C*H*(CH$_3$)$_2$)$_3$), 1.11 (d, 18H, Si(CH(C*H*$_3$)$_2$)$_3$), 0.07 (br s, 5H, B(7−11)−*H*), −0.08 (br s, 1H, B(12)−*H*). ^{11}B NMR (δ, $CDCl_3$): −6.85 (d, 1B, *B(12)*−H, *J*(BH) = 110), −13.17 (d, 10B, *B(2−11)*−H, *J*(BH) = 112). ^{11}B{^{1}H} NMR (δ, $CDCl_3$): −6.85 (s, 1B, *B(12)*−H), −13.17 (s, 10B, *B(2−12)*−H). ^{31}P{^{1}H} NMR (δ, $CDCl_3$): 47.74 (d, *J*(RhP) = 194).

Rh(PPh_3)$_2$(1-Me-9,11,12-(Et)$_3$-*closo*-$CB_{11}H_8$) (10). [(PPh_3)$_2$Rh-(nbd)][1-Me-*closo*-$CB_{11}H_{11}$] (50 mg, 0.057 mmol) was placed in a 15 cm^3 Young ampule, and CH_2Cl_2 (5 cm^3) was added via cannula. The solution was freeze−pump−thawed three times. On the third cycle the solution was warmed to room temperature with stirring under an atmosphere of hydrogen to give [(PPh_3)$_2$Rh(1-Me−$CB_{11}H_{11}$)]. After 30 min excess hydrogen was removed with vacuum and replaced with ethene. After 24 h, the solution was degassed again, hydrogen was placed in the Young ampule, and the solution was stirred for 2 h. This procedure was repeated a total of four times. The solution was then reduced in vacuo to dryness to afford a dark red residue (12 mg, 25%). Crystals suitable for an X-ray diffraction experiment were grown from CH_2Cl_2/pentane solutions. ESI-MS (negative mode): *m*/*z* 241.2, showing the correct isotope pattern for $B_{11}C_8H_{26}$. Compound **10** was always formed with a small (∼10%) of another carborane anion that could not be removed by bulk purification methods. Mass spectroscopy suggests that the identity of this may be [1-H-*closo*-$(C_2H_5)_4$-$CB_{11}H_7]^-$.

^{1}H NMR (δ, CD_2Cl_2): 7.52−7.10 (m, 30H, PPh_3), 1.64 (s, 3H, C_{cage}−C*H*$_3$), 1.02−0.11 (m, 15H, B−C*H*$_2$C*H*$_3$), −4.64 (br q, 2H, B−*H*−Rh). ^{11}B NMR (δ, CD_2Cl_2): −2.1 (vbr, 3B), −12.7 (vbr, 3B), −16.3 (vbr, 3B), −18.8 (d, 2B, *B*−H, *J*(HB) = 94). ^{31}P{^{1}H} NMR (δ, CD_2Cl_2, 298 K): 45.0 (d, *J*(RhP) = 193).

[Rh(PPh_3)$_2$(nbd)][1-Me-9,11,12-(Et)$_3$-*closo*-$CB_{11}H_8$] (11). A solution of [(PPh_3)$_2$Rh(nbd)][1-Me-*closo*-$CB_{11}H_{11}$] (60 mg, 0.068 mmol) in CH_2Cl_2 (10 cm^3) was placed in a 20 cm^3 Young ampule equipped with a magnetic stir bar. The solution was degassed with vacuum and then stirred under an atmosphere of hydrogen to give [(PPh_3)$_2$Rh(1-Me-*closo*-$CB_{11}H_{11}$)]. After 30 min excess hydrogen was removed with vacuum and ethene condensed in (0.259 g). After 4 h, ethene was released, the solution degassed under vacuum again, and the ampule charged with hydrogen. Sequential treatment with ethene and hydrogen as previously described was performed twice more (with reaction times of 16 h and 40 min, respectively). The solvent was evaporated under vacuum and the residue redissolved with CH_2Cl_2. Norbornadiene (0.5 cm^3, 4.63 mmol) was added to the CH_2Cl_2 solution and the mixture stirred for 4 h. The solvent was evaporated under vacuum and the residue redissolved in CH_2Cl_2 (2 cm^3) and precipitated with pentane (15 cm^3) to afford a dark orange precipitate. Solvents were removed by decantation and the product washed with pentane (2 × 4 cm^3) and dried in vacuo to afford the title compound (46 mg, 70.0%) as a dark orange solid. ESI-MS (negative mode): *m*/*z* 241.31, showing the correct isotope pattern for $C_8H_{26}B_{11}$.

^{1}H NMR (δ, CD_2Cl_2): 7.45−7.28 (m, 30H, PPh_3), 4.46 (br s, 4H, C_7H_8), 3.97 (br s, 2H, C_7H_8), 1.56 (s, C_{cage}−*CH*$_3$), 1.53 (br s, 2H, C_7H_8), 1.50 (s, C_{cage}−*CH*$_3$), 0.91−0.42 (m, 15H, B−*Et*). ^{1}H-{^{11}B} NMR (δ, CD_2Cl_2): 7.45−7.28 (m, 30H, PPh_3), 4.46 (br s, 4H, C_7H_8), 3.97 (br s, 2H, C_7H_8), 1.70 (br s, B−*H*), 1.64 (br s, B−*H*), 1.56 (s, C_{cage}−*CH*$_3$), 1.53 (br s, 2H, C_7H_8), 1.50 (s, C_{cage}−*CH*$_3$), 1.44 (br s, B−*H*), 1.38 (br s, B−*H*), 1.33 (br s, B−*H*), 0.91-0.42 (m, 15H, B−*Et*). ^{11}B NMR (δ, CD_2Cl_2): −0.1 (br s, 1B, *B*−Et), −2.3 (br s, 2B, *B*−Et), −8.8 (br s, 1B, *B*−H), −11.2 (br s, 1B, *B*−H), −12.7 (br d, 2B, *B*−H), −13.9 (br d, 2B, *B*−H), −15.9 (br d, 2B, *B*−H). ^{31}P{^{1}H} NMR (δ, CD_2Cl_2, 298 K): 29.4 (d, *J*(RhP) = 155).

[Rh(PPh_3)$_2$(nbd)][1-(^{i}Pr$_3$Si)-9,11,12-(Et)$_3$-*closo*-$CB_{11}H_8$] (12). A solution of (PPh_3)$_2$Rh(1-^{i}Pr$_3$Si-*closo*-$CB_{11}H_{11}$) (179 mg, 0.232 mmol) in CH_2Cl_2 (10 cm^3) was freeze−pump−thawed three times. On the third cycle ethene (∼0.600 g) was added to the solution and the ampule closed and warmed to room temperature. After the solution was stirred for 24 h, it was degassed again, hydrogen was placed in the Young ampule, and the solution stirred for 2 h. This sequential treatment with ethene/hydrogen was repeated a total of three times. Following the last hydrogenation the solvent was degassed and norbornadiene (1 cm^3, 9.27 mmol) added. After the mixture was stirred overnight, the solvent was evaporated under vacuum and the orange residue redissolved in CH_2Cl_2 (2 cm^3) and precipitated with hexane (20 cm^3). The solvent was decanted via cannula and the product dried under vacuum (161 mg, 63%). Anal. Calcd for $C_{59}H_{82}P_2RhSiB_{11}$: C, 64.2; H, 7.49. Found: C, 64.4; H, 7.56. ESI-MS (negative mode): *m*/*z* 383.5 (obsd), showing the correct isotope pattern for $SiB_{11}C_{16}H_{44}$.

^{1}H NMR (δ, CD_2Cl_2, 298 K): 7.50−7.25 (m, 30H, PPh_3), 4.46 (br s, 4H, C_7H_8), 3.97 (br s, 2H, C_7H_8), 1.56 (br s, 2H, C_7H_8), 1.17 (sept, 3H, (Si−(C*H*(CH$_3$)$_2$)$_3$), 1.10 (d, 18H, (Si−(CH(C*H*$_3$)$_2$)$_3$), 0.90-0.40 (m, 15H, B−*Et*). ^{1}H{^{11}B} NMR (δ, CD_2Cl_2, 298 K): 7.50−7.25 (m, 30H, PPh_3), 4.46 (br s, 4H, C_7H_8), 3.97 (br s, 2H, C_7H_8), 1.74 (s, 2H, B−*H*), 1.66 (s, 2H, B−*H*), 1.47 (s, 1H, B−*H*), 1.43 (s, 1H, B−*H*), 1.39 (s, 2H, B−*H*), 1.56 (br s, 2H, C_7H_8), 1.17 (sept, 3H, (Si−(C*H*(CH$_3$)$_2$)$_3$), 1.10 (d, 18H, (Si−(CH(C*H*$_3$)$_2$)$_3$), 0.90−0.40 (m, 15H, B−*Et*). ^{11}B{^{1}H} NMR (δ, CD_2Cl_2, 298 K): 7.7 (br

s, 1B, *B*−Et), −1.4 (br s, 2B, *B*−Et), −10.4 (br s, 1B, *B*−H), −11.9 (br s, 2B, *B*−H), −14.8 (br s, 2B, *B*−H), −16.8 (br s, 3B, *B*−H). $^{31}P\{^{1}H\}$ NMR (δ, CD_2Cl_2, 298 K): 30.5 (d, J(RhP) = 155).

[Rh(PPh$_3$)$_2$(η^2-CH$_2$=CH$_2$)$_3$][*closo*-CB$_{11}$H$_6$Br$_6$] (13). A solution of [(PPh$_3$)$_2$Rh(nbd)][*closo*-CB$_{11}$H$_6$Br$_6$] (20 mg, mmol) in CH_2Cl_2 was freeze−pump−thawed three times. On the third cycle hydrogen (1 atm) was added to the solution to give [(PPh$_3$)(PPh$_2$-η^6-C$_6$H$_5$)-Rh]$_2$[*closo*-CB$_{11}$H$_6$Br$_6$]$_2$.[35] After 30 min the solution was evaporated and the residue dissolved in CH_2Cl_2 under an atmosphere of ethene. Suitable crystals for X-ray diffraction studies were grown at −80 °C by layering ethene-saturated pentane over the CH_2Cl_2 solution. In situ low-temperature $^{31}P\{^{1}H\}$ NMR spectra for the [1-H-*closo*-CB$_{11}$H$_{11}$]$^-$ and [BAr$^F_4$]$^-$ analogues are identical with those of **13**.

^{1}H NMR (δ, CD_2Cl_2, 298 K): 7.60−7.11 (m, 30H, PPh$_3$), 5.2 (excess ethene), 2.59 (br s, 1H, C$_{cage}$−*H*). $^{1}H\{^{11}B\}$ NMR (δ, CD_2Cl_2, 298 K): 7.69−7.11 (m, 30H, PPh$_3$), 5.2 (excess ethene), 2.59 (br s, 1H, C$_{cage}$−*H*), 2.35 (br s, 5H, B−*H*). ^{11}B NMR (δ, CD_2Cl_2, 298 K): −1.55 (s, 1B, *B*−Br), −9.80 (s, 5B, *B*−Br), −20.25 (d, 5B, *B*−H, J(BH) = 156.6). $^{31}P\{^{1}H\}$ NMR (δ, CD_2Cl_2, 298 K): 33.3 (d, J(RhP) = 105). $^{31}P\{^{1}H\}$ NMR (δ, CD_2Cl_2, 238 K): 34.5 (d, J(RhP) = 102).

Acknowledgment. We thank the EPSRC (No. GR/S42750/01) and the Royal Society for funding, Professor Larry Sneddon (University of Pennsylvania) for useful discussions at the beginning of this project, which were enabled by a Royal Society of Chemistry/J. W. T. Jones travelling fellowship awarded to A.S.W., the EPSRC national mass spectrometry service at Swansea University, and Drs. John Lowe and Anneke Lubben at the University of Bath for NMR and mass spectrometric support, respectively. We also thank the reviewers for useful comments.

Supporting Information Available: Text, tables, and figures giving additional experimental and characterization data, full crystallographic data, including bond lengths and angles, for **2a**, **7**, **9**, **10**, and **13**, and ESI-MS spectra for the new complexes. This material is available free of charge via the Internet at http://pubs.acs.org.

OM070043P